heritage

*Article*

# The Condition of Contemporary Murals in Sun-Exposed Urban Environments: A Model Study Based on Spray-Painted Mock-Ups and Simulated Light Ageing

**Varvara Marazioti [1,2,*], Antonios M. Douvas [2], Evangelia C. Vouvoudi [3], Dimitrios Bikiaris [3], Kyriaki Papadokostaki [2], Dimitrios Nioras [2], Evangelos Gogolides [2], Spyros Orfanoudakis [2,4], Thomas Stergiopoulos [2], Stamatios Boyatzis [1] and Yorgos Facorellis [1]**

[1] Department of Conservation of Antiquities & Works of Art, University of West Attica, Egaleo, 12243 Attica, Greece
[2] Institute of Nanoscience and Nanotechnology (INN), National Centre for Scientific Research (NCSR) "Demokritos", Agia Paraskevi, 15310 Attica, Greece
[3] Laboratory of Polymers Chemistry and Technology, Department of Chemistry, Aristotle University of Thessaloniki (AUTh), 54124 Thessaloniki, Greece
[4] Department of Physics, National Technical University of Athens, Zografou, 15780 Athens, Greece
* Correspondence: v.marazioti@gmail.com

**Abstract:** The present work investigates the physicochemical stability of spray paints when irradiated with artificial solar light (at spectral range 300–800 nm). This research highlights the importance of understanding the materials used in street art and public murals, recognising them as a significant component of contemporary cultural heritage. By examining the stability and degradation of spray paints toward solar light exposure, the study aims to contribute to the preservation of contemporary murals, which reflect current social and cultural narratives. A physicochemical approach was employed for the study of spray paints' physical and thermal properties, as well as the effect of specific photochemical ageing reactions/processes. The photochemical ageing results were compared with reference (unaged) samples. Specifically, a multi-technique approach was applied using stereo microscopy, scanning electron microscopy (SEM), atomic force microscopy (AFM), contact angle measurement, colorimetry, glossimetry, differential scanning calorimetry (DSC), UV-Vis spectroscopy, attenuated total reflectance-Fourier transform infrared spectroscopy (ATR-FTIR), and pyrolysis-GC/MS (Py-GC/MS). The photodegradation of the spray paints occurred from the first 144 h of solar light irradiation, resulting in changes in morphology, colour, gloss, roughness, and wettability. Regarding photochemical stability, ageing seems to affect the binders more than the synthetic organic pigments and the inorganic fillers. In particular, acrylic binders showed small chemical changes, whereas the alkyd, nitrocellulose, and styrene binders underwent severe chemical modification. The results suggest that simulated daylight irradiation prompts the migration of additives toward the surface of the spray paint films. In addition, the results of the analyses on the white spray paints in comparison with the coloured paints (from the same manufacturer) showed that there seems to be an active distinct photoageing mechanism involving titanium dioxide, but the whole issue needs further investigation.

**Keywords:** spray paints; accelerated photochemical ageing; photodegradation; solar light irradiation; physicochemical stability

check for updates

**Citation:** Marazioti, V.; Douvas, A.M.; Vouvoudi, E.C.; Bikiaris, D.; Papadokostaki, K.; Nioras, D.; Gogolides, E.; Orfanoudakis, S.; Stergiopoulos, T.; Boyatzis, S.; et al. The Condition of Contemporary Murals in Sun-Exposed Urban Environments: A Model Study Based on Spray-Painted Mock-Ups and Simulated Light Ageing. *Heritage* **2024**, *7*, 3932–3959. https://doi.org/10.3390/heritage7080186

Academic Editor: Maurizio Aceto

Received: 8 July 2024
Accepted: 26 July 2024
Published: 30 July 2024

**Copyright:** © 2024 by the authors. Licensee MDPI, Basel, Switzerland. This article is an open access article distributed under the terms and conditions of the Creative Commons Attribution (CC BY) license (https://creativecommons.org/licenses/by/4.0/).

## 1. Introduction

Urban murals have conquered public space worldwide [1] and are widely considered a highly significant and inseparable part of the contemporary cultural heritage [2]. Due to their exposure to external environmental conditions [3], anthropogenic factors, and the overall ephemeral character of contemporary paints [1], signs of significant deterioration

such as loss of cohesion, loss of material (scaling, peeling, craquelure), discolouration, biological colonisation, abrasion, vandalism, etc. raise concerns about their preservation status and conservation treatments [2,3].

Contemporary paints are mainly based on acrylic, alkyd, polyvinyl acetate, and cellulose nitrate binding media [4,5]. During the last decades, several research studies have focused on the stability of synthetic binders in the field of cultural heritage [6]. However, the behaviour of outdoor paints over time and the conservation guidelines have been scarcely investigated, a fact quite challenging for the conservation of modern and contemporary artworks, such as urban murals [2,7]. Thus, determining the factors influencing their ageing behaviour, especially regarding materials exposed to outdoor conditions, and developing appropriate conservation practices have become crucial to heritage science today [4,8].

External environmental factors (namely temperature, relative humidity, solar light irradiation, pollutants, etc.) considerably influence the physicochemical deterioration of synthetic polymers [9]. In general, organic polymers are photodegraded, with or without the presence of oxygen, via photolysis, photo-oxidation, and/or photoreduction [7]. One of the most severe degradation agents of synthetic polymers in the outdoor environment is solar light irradiation, which, in the presence of oxygen, promotes photo-oxidation reactions (i.e., chain scission and cross-linking reactions that produce a series of reactive intermediates and radicals) of polymers [1,8]. These reactions are influenced by high temperatures and relative humidity and, especially, by the presence of atmospheric pollutants [10]. Likewise, the presence of catalyst residues and/or other impurities may initiate photo-oxidation [11]. Photodegradation processes begin with photon absorption by the polymer macromolecules and subsequent breaking of chemical bonds and generation of polymer alkyl radicals (initiation step) [8]. Next, radical chain reactions (propagation step) occur until new non-radical products are produced by the recombination of radicals (termination). Cross-linking of polymer chains occurs as a result of macroradical recombination [8].

Most studies have dealt with UV ageing of synthetic paints in indoor museum conditions at wavelengths between 400 and 315 nm ($UV_A$), while the influence of $UV_B$ light (315–280 nm), which could give valuable information on the stability of artworks exposed to outdoor conditions, is examined to a lesser extent [4]. $UV_B$ (5–10% of solar light) radiation causes crack formation, discolouration, loss of gloss, chalking, embrittlement, stiffening, changes in solubility, etc. [4,8,11,12], while $UV_A$ (90–95%) is considered less harmful to polymers [1,11,12], and $UV_C$ radiation (280–100 nm) is absorbed by the atmosphere [4,12]. In addition, most scientific research has been focused on the degradation mechanisms of water-based acrylic dispersions and not on organic solvent-based ones, such as spray paints, which are mostly acrylic or alkyd solutions in a mixture of organic solvents [12].

(Meth)acrylic binders used in contemporary paintings derive from the polymerisation of (meth)acrylic esters [13]. Solvent-borne and water-based acrylic binders are prone to photo-oxidation reactions, which are mostly scission reactions of the main chains, scission of the side ester groups, cross-linking of the polymer backbone, and formation of decomposition compounds (hydroperoxides, alcohols, ketones, anhydrides, $\gamma$-lactones) [1,4,6,14,15]. Furthermore, the carbonyl groups present in the acrylic structure are also sensitive to secondary photodegradation reactions, such as Norrish-type reactions [8,16,17]. When the side ester group is short ($C_1$–$C_3$), main chain scission reactions prevail over cross-linking ones, whereas when it is long ($\geq C_4$), the polymers undergo fast and extensive cross-linking through scission of the side ester group and recombination of macroradicals [10]. The photo-oxidation starts first in the uppermost layer of the paints and proceeds toward the bulk, depending on the radiation wavelength range, exposure time, oxygen diffusion, etc. [8]. In general, methacrylic polymers are more stable toward photo-oxidation than acrylics since the presence of methyl groups on the polymeric backbone slows down hydrogen abstraction reactions and, therefore, the subsequent photodegradation of the polymer [7,10,14,18].

Alkyd binders are oil-modified alkyd polyesters resulting from the condensation polymerisation of polyols, dicarboxylic acids, and monobasic fatty acids [4,19,20]. The

highly branched polyester backbone becomes more flexible with the addition of a fatty acid, which reduces the cross-linking [19]. However, it has been proven that the fatty acid component constitutes the main deterioration agent in long-oil alkyds, as the oxidation processes continue after the film formation [20]. The drying process of films is catalysed by auto-oxidation reactions (chemical drying) that take place after solvent evaporation (physical drying) [19–21]. Auto-oxidation usually follows a free-radical reaction mechanism, which comprises the oxidative cross-linking of the unsaturated fatty acid side chains toward the formation of hydroperoxides (ROOH) [21,22]. The terminal products can further react with radicals to increase molecular weight, resulting in excessive cross-linking and chain scission ($\beta$-scission degradation) [22]. $\beta$-scission leads to the formation of oxygenated species, including aldehydes, alcohols, and carboxylic acids, as well as peroxy radicals, which may react, forming more cross-links or carboxylic acids through hydrogen abstraction [1,20,23]. Depending on the position of the $\beta$-scission reactions, the fragments can be converted into free low-molecular-weight compounds, which either remain in the polymer matrix unreacted or cross-linked with macromolecules or can be removed by evaporation [4,20]. The evaporation of the low-molecular-weight compounds renders the paint surface relatively enriched in pigment content. As a result, the bands associated with pigments increase in intensity with ageing [24,25]. Auto-oxidation results in excessive cross-linking (stiff and brittle films), chain scission, loss of volatile products (aldehydes, alcohols, carboxylic acids), fading, and discolouration (yellow or brown) [1,4,20]. Another issue is the photo-oxidative reactions of Norrish type I, i.e., cleavage of an $\alpha$ carbon of polyketones and polyesters and formation of peroxy radicals, which may react toward oxidative ageing. Furthermore, there are also the photo-oxidative reactions of Norrish type II, i.e., cleavage of a $\gamma$-hydrogen of polyketones and polyesters and formation of double bonds ($\beta$-elimination), which can also be photolysed [22].

Acrylic and alkyd binders are often co-polymerised with styrene, as they increase the glass transition temperature of polymers while reducing the cost of the formulation [26]. In addition, silver spray paints are usually based on polystyrene binding media. However, polystyrene makes the film more susceptible to UV radiation, and as a result, styrene-modified acrylic binders are more prone to photo-oxidation than pure acrylics [15,26].

Nitrocellulose is another binder found in many spray paints. Nitrocellulose (NC) or cellulose nitrate is one of the oldest cellulose derivates used as a binder in paints [27]. NC is the polynitrate ester of cellulose, a polysaccharide composed of pyranose rings [28,29]. It has been found to be particularly susceptible to both thermal and photochemical degradation, the latter in the wavelength range of 360–400 nm [28,29]. Although the thermal decomposition phenomena of NC have been widely investigated, the photodegradation of NC has received considerably less attention [28]. The photo-oxidation of NC has been described as an autocatalytic process involving a two-step decomposition process [30]. During primary decomposition, $NO_2$ is released from NC (de-nitration), followed by the formation of oxidation products. During secondary decomposition, the oxidised NC products react, resulting in chain scission of the cellulosic backbone. In addition, a major reduction in the molecular weight of NC correlated with the loss of pyranose and acetal groups has been observed [28,30,31]. Eventually, UV radiation causes discolouration of NC (to yellow or brown colour), while the slow loss of volatile stabilisers and plasticisers results in embrittlement of the films, which are characterised by poor mechanical and physical properties (strength and toughness) [32,33].

Overall, research has shown that alkyd paints are more susceptible to UV degradation than acrylics [12]. Polystyrene binders are the least photostable [7].

Another issue is the co-existence of other compounds present in paints, which can influence the degradation of polymers [14]. In particular, inorganic pigments may act protectively by absorbing UV light, or they may be photoactive and thus accelerate the photodegradation of polymers [1,4,6,8,14]. Such an example constitutes the $TiO_2$ found in different crystalline phases (rutile, anatase, or both), which have been reported to either stabilise the binders or facilitate their degradation [12,15,34]. Furthermore, synthetic organic

pigments (SOPs) are usually susceptible to photo-oxidation themselves, so they seem to contribute to the overall photoageing behaviour of paints with mechanisms that are poorly understood [4,8,35]. For example, dioxazine pigment PV37 acts as a stabilising agent for styrene acrylic binders, while PB15:1 promotes degradation processes [5]. Additionally, the photodegradation of the pigments depends on the chromophore type and concentration [7].

Last but not least, photodegradation is also influenced by the film thickness and the radiation wavelength range. For instance, alkyd paints degrade more under $UV_A$ radiation, whereas acrylics under $UV_B$ [7].

Furthermore, although the lifespan of the paints is precisely estimated based on field exposure tests, they are quite time-consuming. Due to this, accelerated ageing is typically employed [26], as it has proven to be a valuable tool for evaluating the durability of polymeric materials and predicting their long-term behaviour [36]. Particularly in paints, artificial ageing focuses on the effects of irradiation, temperature, relative humidity (RH), salts, etc. [36]. It should be noted that although paints have been investigated in photoageing experiments in the past, it is difficult to draw conclusions, as the experiments were conducted under different experimental conditions, including photo ageing parameters (i.e., different light intensity and wavelength range, etc.) [15].

In the opinion of the authors, there is a considerably increasing research interest in the contemporary art conservation community concerning the solar light ageing and deterioration processes of artists' spray paints [1,3,7,12,36–38]. In this context, this paper investigates the stability of a range of spray paints containing different binding media, synthetic organic pigments, inorganic fillers, and other additives before, during, and after accelerated solar light ageing (totally 710 h) through physicochemical analysis. In particular, the present work investigates the effect of solar light on the physical stability of spray paint (morphology, colour, gloss, contact angle), as well as on the photochemical and thermal stability of these complex systems, along with the product formation by their degradation upon pyrolysis. Additionally, the research gives important information on the lifetime of spray paint materials by monitoring changes that occurred during outdoor photochemical ageing.

## 2. Experimental

### *2.1. Materials*

The spray paints selected in this study were obtained from three manufacturers (Flame Blue, Montana Black, and Montana Gold) in five colours (white, black, red, green, and blue), as presented in Table 1. The brands and colours were chosen as representative media used by Greek street artists. The exact description (code names) of the samples is provided to support possible future conservation studies. The samples have been previously analysed using ATR-FTIR, Raman spectroscopy, and SEM-EDS in a recent work of the authors [39], and all the information is briefly presented in Table 1.

**Table 1.** Spray paints investigated in this study.

| Sample ID | Manufacturer —Colour | | Code Names | Composition | | |
|---|---|---|---|---|---|---|
| | | | | Binder * | Synthetic Organic Pigments | Inorganic Pigments and Fillers |
| **FB_W** | Flame White | Blue | FB-900 Pure White | P(*n*BMA-MMA)/NC | | PW6 PW19 PW21 PW26 |
| **FB_Bk** | Flame Black | Blue | FB-904 Deep Black | P(*n*BMA-MMA)/NC | | PW6 PW19 PW26 |
| **FB_R** | Flame Red | Blue | FB-312 Fire Red | P(*n*BMA-MMA)/NC | PR254 | PW6, PW19 PW21 PW26 |
| **FB_G** | Flame Green | Blue | FB-630 Fern Green | P(*n*BMA-MMA)/NC | PB15:1 PG7 PY74 | PW6 PW18 PW19 PW21 PW25 PW26 |
| **FB_B** | Flame Blue | Blue | FB-512 Signal Blue | P(*n*BMA-MMA)/NC | PB15:1 | PW6 PW19 PW21 PW26 |

**Table 1.** *Cont.*

| Sample ID | Manufacturer —Colour | Code Names | Composition | | |
|---|---|---|---|---|---|
| | | | Binder * | Synthetic Organic Pigments | Inorganic Pigments and Fillers |
| **MB_W** | Montana Black —White | BLK400-9105 White | Alkyd/NC/Sty | | PW6 PW18 PW19 PW21 PW25 PW26 |
| **MB_Bk** | Montana Black —Black | BLK409-9001 Black | Alkyd/NC/Sty | | PW6 PW19 PW21 PW26 |
| **MB_R** | Montana Black—Red | BLK400-2093 Code Red | Alkyd/NC/Sty | PR112 | PW6 PW19 PW21 PW26 |
| **MB_G** | Montana Black —Green | BLK460-6055 Boston | Alkyd/NC/Sty | PG7 PY74 | PW6 PW19 PW21 PW26 |
| **MB_B** | Montana Black—Blue | BLK400-570 Horizon | Alkyd/NC/Sty | PB15:6 | PW6 PW19 PW21 PW26 |
| **MG_W** | Montana Gold—White | S9100 Sh. White | P(*n*BMA-MMA)/NC/Sty ** | | PW6 PW19 PW21 |
| **MG_Bk** | Montana Gold— Black | S9000 Sh. Black | P(*n*BMA-MMA)/NC/Sty ** | | PW19 PW26 |
| **MG_R** | Montana Gold—Red | S3000 Sh. Red | P(*n*BMA-MMA)/NC/Sty | PR112 | PW6 PW19 PW26 |
| **MG_G** | Montana Gold—Green | S6020 Sh. Green Dark | P(*n*BMA-MMA)/NC/Sty ** | PG7 PY74 | PW6 PW19 PW21 |
| **MG_B** | Montana Gold—Blue | S5010 Sh. Blue | P(*n*BMA-MMA)/NC/Sty ** | PB15:6 | PW6 PW19 PW21 PW26 |

* *n*BMA: *n*-butyl methacrylate; MMA: methyl methacrylate; NC: nitrocellulose; Sty: styrene. ** The MG samples were found in the present work through ATR-FTIR and Py-GC/MS to possibly also have an alkyd binder (pls. see below).

### 2.2. Accelerated Daylight Ageing

The accelerated solar light ageing of the samples was conducted in a Suntest XLS+ (Atlas Material Testing Technology, Mt Prospect, IL, USA)), equipped with a xenon-arc lamp, which provides constant radiation within a wavelength range between 300 and 800 nm at a power of 765 W/m$^2$, simulating outdoor sunlight conditions. The black-standard temperature was set at 65 ± 3 °C, according to [40]. Relative humidity (RH) and temperature (T) were not customisable in the specific UV chamber; therefore, the RH (~58%) and T (~22 °C) varied depending on the ambient conditions in the lab. Air contaminants are uncontrollable environmental factors. After their initial chemical characterisation and the investigation of their physical properties, the specimens were arranged in the chamber and exposed totally to solar light radiation for 710 h (total irradiation dose = 276.048 MJ/m$^2$). Changes in chemical, physical, and thermal properties of the spray paint layers were assessed using contact angle measurement, colorimetry, gloss, and ATR-FTIR (every 144 h), and stereo microscopy, SEM examination, AFM, DSC, and Py-GC/MS (at the beginning and the end of the photoageing process).

### 2.3. Sample Preparation—Substrates

For stereo microscopy, SEM, AFM, ATR-FTIR, and Py/GC-MS analyses, the samples were prepared by spray painting on Teflon sheets (~2 × 2 cm$^2$, 1 mm thickness), maintaining a constant pressure, from ~20 cm distance and after 2 min of shaking. For contact angle measurement, colorimetry, and gloss, the samples were produced via spray painting on glass slides (2.5 × 7.5 cm$^2$, 1 mm thickness). For UV-Vis spectroscopy, the samples were studied in the form of thin films of uniform thickness on quartz slides (~2 × 2 cm$^2$, 1 mm thickness). In this case, each spray paint sample was prepared by spin coating of 10% (*w*/*w*) spray paint dispersions/solutions in tetrahydrofuran (THF) on quartz slides at 3000 rpm for 120 s (Headway Research INC model No CR15). Lastly, for DSC analysis, a quantity of ~12 mg of each spray paint was deposited into small aluminium pans using syringes. For the measurements before accelerated ageing, the pans were sealed after being left to dry at room temperature for a month, a time considered sufficient for the complete evaporation of the volatile organic solvents used in spray paint formulations. For the measurements after artificial ageing, the pans were placed in the chamber without covers, irradiated, and sealed after the end of the ageing procedure.

A variety of substrates (i.e., Teflon sheets, glass slides, and quarts slides) was used depending on the characterisation technique applied. This was done even though the actual degradation processes of the spray paint films take place on wall supports because the rationale of the present research was to investigate the physicochemical effect of spray paints' photochemical ageing regardless of the substrate [7,15]. Lastly, two identical samples (replicated) for each colour and company were prepared to allow statistical evaluation of results.

### *2.4. Methods*

Before, during, and after the artificial solar light ageing, the spray paint specimens were subjected to characterisation to monitor the physical, thermal, and chemical modifications caused by the photodegradation process.

#### 2.4.1. Stereomicroscopy

The samples were examined under an SZ61 Zoom Stereomicroscope (Olympus LS, Tokyo, Japan) using reflected/transmitted light LED illumination at a magnification range extending from 6.7× to 45× (using 10× eyepieces), to observe changes in the morphology of the spray paint films caused by the ageing procedure. The stereomicroscope is equipped with a Lumenera INFINITY1-2CB 2.0 megapixel Scientific USB 2.0 CMOS Camera (Lumenera Corporation, Ottawa, ON, Canada). Images were processed using the INFINITY ANALYZE v.6.5.6 software.

#### 2.4.2. Scanning Electron Microscopy (SEM)

The morphological examination was conducted at different magnifications in the range 100–2000×, using the scanning electron microscope (SEM/EDS) JEOL JSM 6510 LV SEM (JEOL ltd., Akishima, Tokyo, Japan), operated in a low-vacuum mode of 40 Pa, in BSE mode (backscattered electron detector), and at an accelerating voltage of 20 kV.

#### 2.4.3. Atomic Force Microscopy (AFM)

AFM is a non-invasive imaging technique that offers significant information (i.e., roughness, particle sizes, etc.) on the surface morphology of polymeric materials [41,42]. The analysis was performed on unaged samples ($t_0$) and fully photoaged samples ($t_f$), i.e., after 0 h and 710 h of irradiation doses, respectively. The analyses were conducted using anatomic force microscope, SOLVER NANO (NT-MDT Spectrum Instruments Co., Moscow, Russia), in contact mode using the CSG30 tips, having a constant force of about 0.6–2 N/m and a resonance frequency of about 26–76 kHz. Images were recorded with 256 × 256 pixels resolution and an area of 50 × 50 $\mu m^2$. Nova Px 3.4.1 software was employed for data acquisition and manipulation. The images were shown in false colour, where brighter areas represented higher areas. The surface morphology of the samples was characterised by the arithmetical mean surface height ($S_a$) and the average maximum profile height-root mean square ($S_q$). Furthermore, information about the unaged and aged surfaces was given by the parameter $S_{dr}$ (developed interfacial area ratio), which is defined as the ratio between the interfacial and the projected solid surface area. A completely flat surface would have an $S_{dr}$ value of 0% [43]. The roughness ratio $r$ can be calculated according to the following equation:

$$r = 1 + \frac{S_{dr}}{100} \quad (1)$$

#### 2.4.4. Contact Angle Measurement

Contact angle measurement is one of the quickest methods for determining surface changes in paints [20], especially in terms of wettability (hydrophilicity/hydrophobicity) evaluation [3]. The measurements were performed according to [44], using a Krüss Drop Shape Analyzer DSA100E instrument (Krüss Scientific Instruments, Hamburg, Germany) equipped with a high-speed camera and the Advance Krüss software v.1.14. The shape

of a 5 μL water drop was documented through photography. For each sample, three measurements on three different points were conducted. For the evaluation of the $\theta$ angle, the values were averaged and the standard deviation was calculated.

#### 2.4.5. Colorimetry

The colourimetric measurements of the specimens before and after artificial photochemical ageing were performed using a PCE-CSM colourimeter (PCE Instruments UK Ltd., Manchester, UK) over a white surface (reflectance $\geq$ 95%). The measurements were collected using a standard illuminant (light source) D65 with an observer at 10° and an aperture diameter of 8 mm. For the acquisition of the colour coordinates, the measurements were collected in both specular components included (SCI) and excluded (SCE) modes since both provide significant information about the morphological changes [3]. The evaluation of the colour changes was conducted using the CIE LAB, LCh Color Space, and the CIE 1976 Color Formula and expressed as $\Delta E^*$, which was determined according to Equation (2) [45,46] as follows:

$$\Delta E^* = \sqrt{\Delta L^{*2} + \Delta a^{*2} + \Delta b^{*2}} \quad (2)$$

where $L^*$ represents lightness increasing from zero (absolute black) to 100 (absolute white); $a^*$ is associated with the modification in redness/greenness (positive $a^*$: red, negative $a^*$: green); and $b^*$ is associated with the changes in yellowness/blueness (positive $b^*$: yellow, negative $b^*$: blue) [12,47].

The higher $\Delta E^*$ values indicate the most visible colour changes. When the $\Delta E^*$ values are >5 CIELab units, then the chromatic alteration is visually perceptible [6,7]. For each sample, the average of three measurements on six different points was calculated. Values were averaged and the standard deviation was calculated. The acquisition of the measurements was conducted using the SQC8 software v.1.9.1.

#### 2.4.6. Gloss Measurement

Gloss measurements of both unaged and aged spray paint films were conducted with a Novo-Gloss 20/60/75° gloss meter (Rhopoint Instruments Ltd., East Sussex, UK), collecting three incidence angles simultaneously. The change ($\Delta G$) was determined considering the gloss value of unaged samples as the reference. Values were shown as the average of three readings per sample $\pm$ standard deviation. Final values were obtained mainly using the reflection angle of 60° according to [47,48]. Any glossiness difference greater than 5 GU is noticeable to the naked eye.

#### 2.4.7. Differential Scanning Calorimetry (DSC)

Differential scanning calorimetry (DSC) has been widely used in the field of cultural heritage as it has been proven a valuable technique for the investigation of thermal properties, especially the glass transition temperatures ($T_g$) of polymeric materials. When the ambient temperature is below $T_g$, the material is in a glassy state, whereas above $T_g$, it is in a rubbery state. Consequently, any modification of $T_g$ due to photochemical ageing could indicate whether the material becomes brittle or tacky. Changes in $T_g$ values are considered indicative of photo-oxidation of polymeric materials. Additionally, DSC has been used to examine the influence of binders (and pigments, additives, etc., as well) on the overall ageing behaviour of the spray paint film based on the shape of the thermal analysis curve [49].

The thermal behaviour of the spray paints was examined with temperature-modulated DSC by determining the $T_g$ of these materials before and after the photochemical ageing. DSC measurements were conducted with the 2920 Modulated Differential Scanning Calorimetry instrument (TA Instruments, New Castle, DE, USA). One heating run was performed in a nitrogen environment from −20 °C to 200 °C (Flame Blue) or −40 °C to 200 °C (Montana Black and Montana Gold) with a scanning rate of 5 °C/min, and tem-

perature modulation of ±0.796 °C every 60 s. Temperature-modulated DSC allows the deconvolution of the total signal (corresponding to conventional DSC) in reversing and non-reversing components [50]. The $T_g$ was calculated from the reversing TMDSC signal using Universal Analysis Software v.4.5A.

#### 2.4.8. UV-VIS Spectroscopy

UV-Vis spectroscopy was employed as it has been proven to be a useful method to detect degradation processes on polymeric materials [51], such as changes in chromophore groups due to photoageing [52]. The absorption spectra were collected using a PerkinElmer UV-Vis Lambda 40 spectrophotometer (PerkinElmer, Waltham, MA, USA) at a wavelength range of 190–900 nm, scan speed 200 nm/min, data interval 1 nm, and slit width 2 nm. The data were collected with the UV WinLab v.285.04 software and were further processed with the OriginPro 2023 v.10.0.0.154.

#### 2.4.9. Attenuated Total Reflectance-Fourier Transform Infrared Spectroscopy (ATR-FTIR)

ATR-FTIR was employed in this work because it is a suitable method for investigating changes in the chemical bonds of polymeric materials (including binders, organic pigments, and fillers) during photochemical processes, such as photo-oxidation [8]. The analysis of the artificially photoaged samples was conducted on a Bruker Alpha II FT-IR (Bruker Corporation, Billerica, MA, USA), equipped with a Bruker diamond crystal ATR spectrometer (manufacturer's spectral range 7500–400 $cm^{-1}$), in absorbance mode, in the 4000–400 $cm^{-1}$ region, at a resolution of 4 $cm^{-1}$, and by summing 50 scans. The spectra were recorded on Bruker OPUS v.8.5 software and were further processed on Spectragryph-optical spectroscopy software, v.1.2.16. Baseline correction and normalisation at 465 $cm^{-1}$ (Fe oxides), 675 $cm^{-1}$ ($TiO_2$), or 870 $cm^{-1}$ ($CaCO_3$) were applied in all spectra, assuming that these bands were not affected during the photoageing process.

#### 2.4.10. Pyrolysis-Gas Chromatography/Mass Spectrometry (Py-GC/MS)

The analytical technique chosen to identify the degradation products of the spray paint s before and after the photoageing process was Py-GC/MS. The pyrolysis step breaks the polymer into simpler fragments under a certain temperature, which (fragments) enter in a GC/MS. An EGA/PY-3030D multi-shot pyrolyser and CGS-1050Ex carrier gas selector (Frontier Laboratories, Fukoshima, Japan) were used in conjunction with a QP-2010 UltraPlus GC/MS analyser (Shimadzu, Fukoshima, Japan) under He gas constant flow. The conditions of the method applied had been previously developed [53]. Tiny quantities of the samples were required without pre-treatment. A glass capillary column consisting of 95% dimethylsiloxane (30 m × 0.25 mm (i.d) × 0.25 μm) MEGA-5HT (Column ID#171734, Italy) was used for chromatographic separation. Tiny quantities of each sample were placed directly into cylindrical stainless steel cups and pyrolysed for 0.5 min at 400 °C. The oven heat program was as follows: initial temperature at 50 °C for 1 min, heating from 50 to 300 °C with a heating rate of 10 °C/min, and final constant temperature for 4 min. The total program time was set at 30 min, and the interface temperature at 200 °C. The ion source worked at 200 °C, the mass range detected was between 30 and 500 amu, the data were taken every 0.1 s, and the detector voltage was at 1.2 kV. The He circulated with a continuous column flow of 1 mL/min and purge flow of 3 mL/min, total flow at 104 mL/min, inlet pressure at 53.5 kPa, linear velocity at 36.3 cm/s, and the split ratio at 1:50. The software used was GCMS post-run analysis and the library for identification was NIST (Shimadzu 2011). The peaks' integration parameters were slope 2000 $min^{-1}$, width 3 s, drift 4000 $min^{-1}$, T.DBL 10,000 min. The analyses results after chromatographs' processing gathered 55–130 peaks, whose main peaks, in terms of intensity (A/H ratios), were presented.

## 3. Results and Discussion

Initially, it is important to mention that the investigation of the aforementioned spray paints' photoageing poses several challenges that make the interpretation of results quite difficult. These challenges arise from a variety of factors, which are mainly the following. (a) Compositional inhomogeneity: The spray paint films vary in composition (i.e., different pigments, binders, additives, concentrations, etc.). This variation can significantly affect the solar light ageing of the spray paint film. (b) Surface texture: The smoothness or roughness of spray paint films can considerably influence light absorption by these films. Different textures may lead to variation in photoageing effects. (c) Particle size and distribution: The size and distribution of particles (which are mainly pigments and fillers) within the spray paint films can also impact the absorption of light by the films. Variations in particle characteristics can even significantly affect the photoageing reaction course within the spray paint films. (d) Film thickness: The thickness of the spray paint film can considerably affect the absorption of light (mainly the uniformity of light absorption) by these films. The different film thicknesses may result in different degrees and extents of photoageing within the spray paint film. Despite the difficulties from these factors, the effect of the accelerated photoaging of spray paints on their physicochemical properties was investigated using the following methods.

### *3.1. Morphological Examination with Stereomicroscopy, SEM, AFM*

Minor spray paint deterioration as a result of accelerated photoaging was evident from the data collected through the microscopic examination. More specifically, after 710 h of solar light exposure, colour fading and changes in surface gloss were observed in the majority of the samples, whereas other samples did not show relevant changes. In general, the aged spray paint layers were characterised by high amounts of polymer binder with well-embedded pigments and fillers in the polymer matrix, judging by the homogeneous surfaces observed. Nevertheless, in some cases, the aged samples exhibited increased roughness (e.g., the MG_B sample, Figure 1a), whereas, in others, ageing seems to have resulted in smoother surfaces (e.g., the MB_Bk sample, Figure 2a). These considerations are confirmed by SEM (Figures 1b and 2b) and AFM 2D and 3D analyses (Figures 1c,d and 2c,d). Unfortunately, the surface roughness of the aged spray paints cannot be correlated with the type of binder and seems to be random. However, this issue needs further investigation.

The main deterioration process observed by SEM was the migration of some components from the bulk of the spray paint layer to the surface. This phenomenon could be a consequence of binder degradation, which leads to the exposure of inorganic compounds [54,55]. However, EDS analysis did not reveal any differentiation in the chemical composition. Thus, these substances may be attributed to organic pigments and/or additives moved to the surface [56].

Regarding AFM analysis, a linear texture profile was observed in all cases, with a mean distance between repeated features to be in the order of 30 μm. Both $S_a$ and $S_q$ parameters increased for some samples, whereas in other cases, surface roughness decreased, but not significantly, compared with the pristine samples. This phenomenon has been mentioned by other researchers, although in different chemical systems (i.e., emulsion water-based paints) [18,42]. On the other hand, binder degradation causes an increase in surface roughness [57]. The average $S_{dr}$ parameter was estimated at ~1.4% for the unaged samples and ~17% for the aged samples. The increased $S_{dr}$ values could be attributed to the increased particle size, possibly due to extruded particles (pigments or fillers) to the surface of the paints and the relatively lower binder content [58]. In general, photodegradation of the binders results in the enrichment of the surface of aged paints with white inorganic fillers and/or organic additives. Thus, increased surface roughness and gloss changes in aged paints are observed [8].

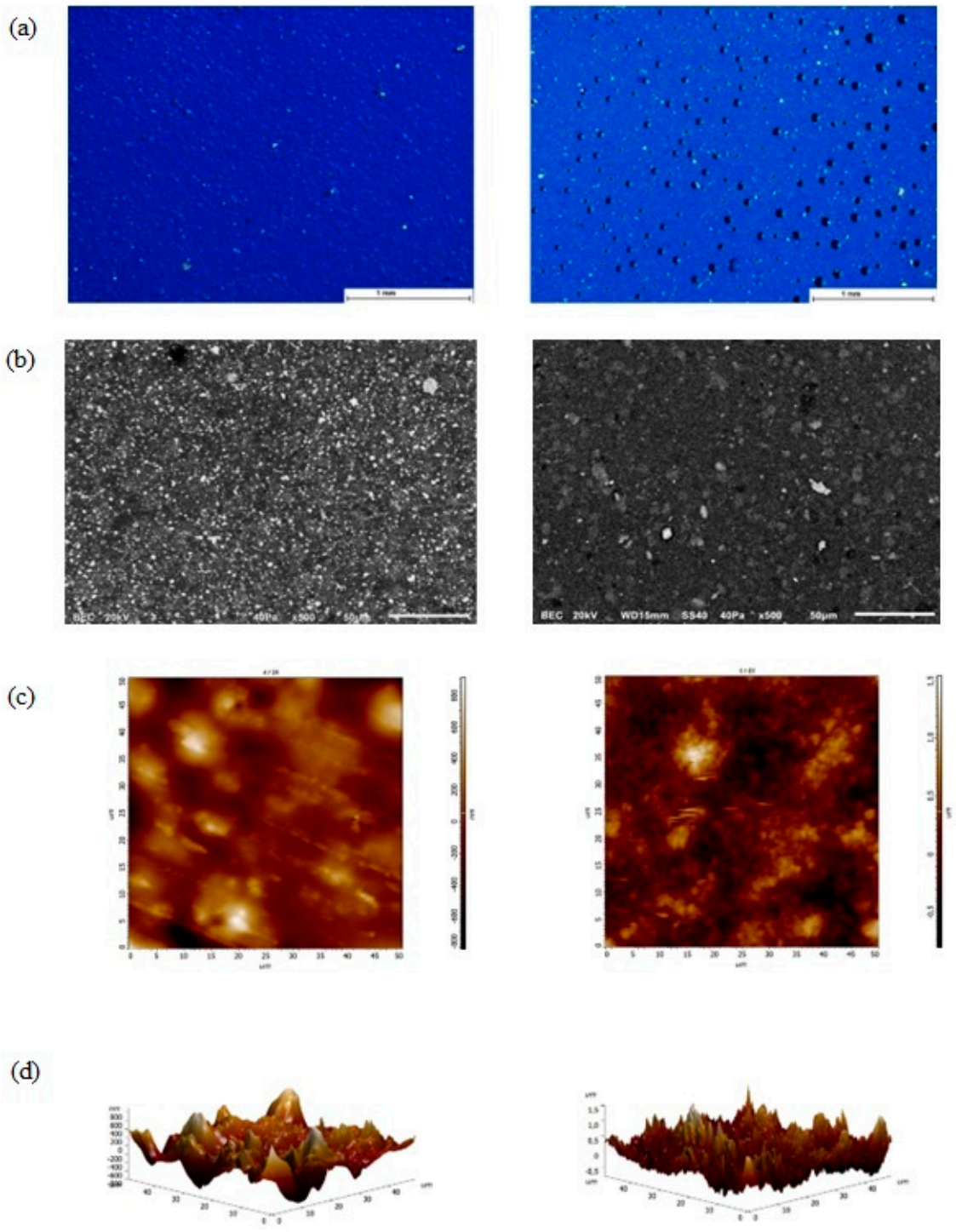


**Figure 1.** (**a**) Stereomicroscopic images (100×), (**b**) backscattered SEM images, (**c**) AFM 2D images, and (**d**) AFM 3D images of the MG_B sample. The unaged ($t_0$ = 0 h) and photoaged ($t_f$ = 710 h) samples are shown on the left and right sides, respectively.

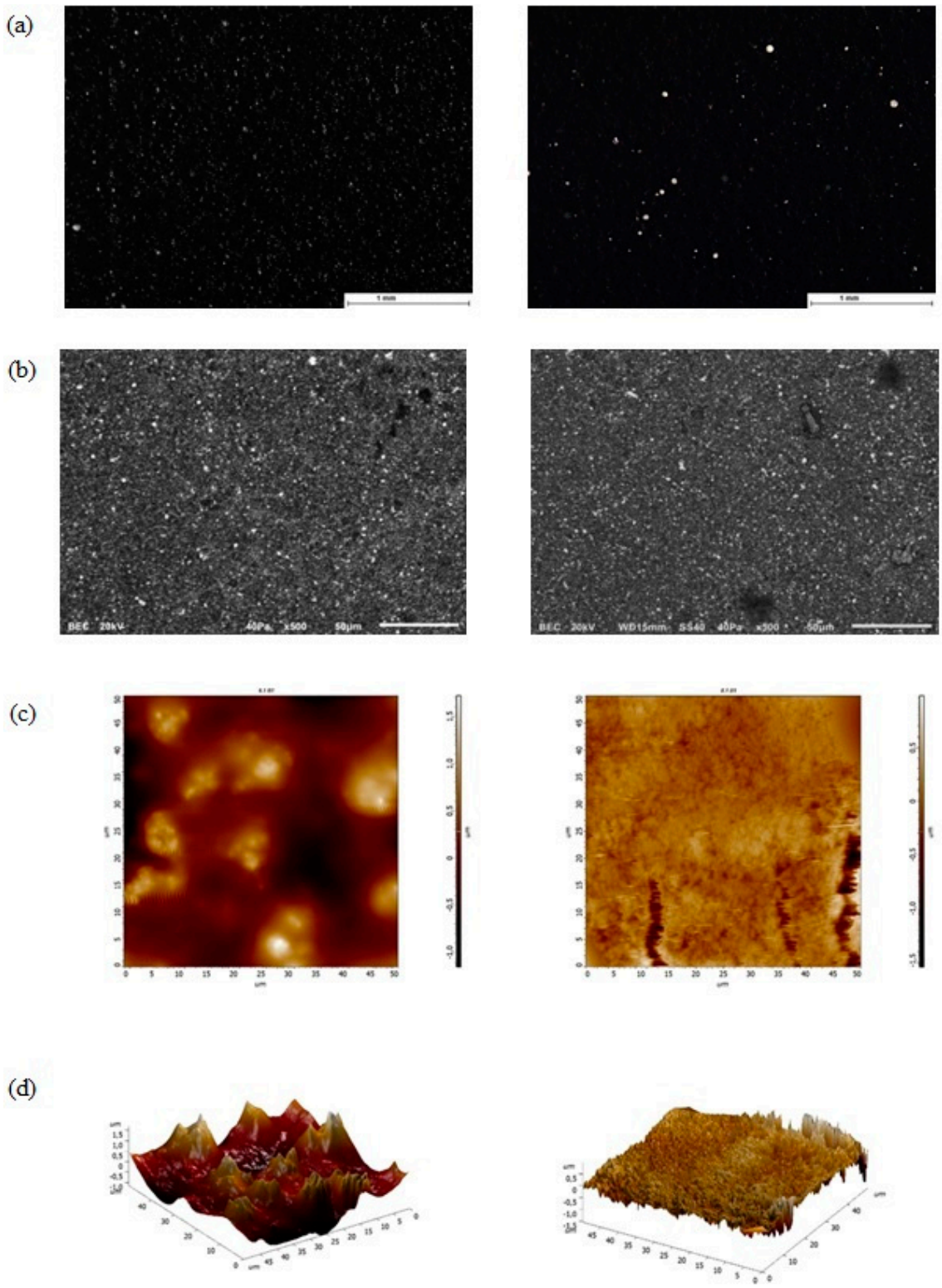


**Figure 2.** (**a**) Stereomicroscopic images (100×), (**b**) backscattered SEM images, (**c**) AFM 2D images, and (**d**) AFM 3D images of the MB_Bk sample. The unaged ($t_0$ = 0 h) and photoaged ($t_f$ = 710 h) samples are shown on the left and right sides, respectively.

### *3.2. Contact Angle Measurement*

A common aspect in almost all samples, except for the MB_B sample and the Montana Gold spray paints, which were initially hydrophobic ($\theta \sim 99°$), is that prior to the artificial

daylight exposure, the contact angles were between 79 and 89°, corresponding to partial hydrophilic surfaces (Chart 1) [7,19]. After artificial daylight exposure of spray paints, there was a decrease in $\theta$ values, i.e., the affinity with water increased. The increased hydrophilicity may be caused by the formation of new species, possibly derived from the binder and containing oxygen [19]. Moreover, the surfaces became more hydrophilic and rougher, since the hydrophilic substances present in spray paints (such as talc) are extruded to the surface of the paints [3,7]. The MB_W sample proved to be the most hydrophilic ($\theta$ = 4°) after solar light ageing, whereas the MG_B sample presented the least amount of modification ($\Delta\theta$ = 20°).

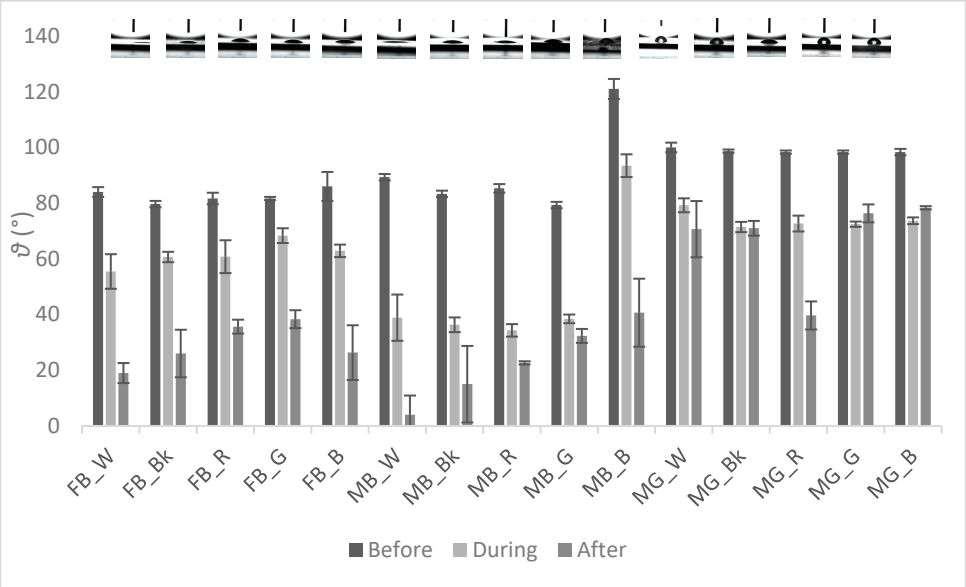


**Chart 1.** Contact angle values of spray paint samples before (0 h), during (432 h), and after accelerated solar light ageing (710 h), accompanied by sessile-drop photographs captured at the end of the ageing. Error bars show the standard deviation.

### *3.3. Colorimetry*

Chromatic profile alterations of spray paint layers due to solar light ageing are illustrated in Charts 2 and 3. Tables S1 and S2 summarise the colour variations of the investigated spray paints, including the shifts in the values of lightness/darkness ($L^*$), redness/greenness ($a^*$), yellowness/blueness ($b^*$), total colour ($E^*$), chroma ($\Delta C^*$), and hue ($\Delta h^*$). The general trend observed in colour measurements was an increase in the $\Delta E^*$ values during the first 144 h of solar light irradiation corresponding to brightening/fading of paints [4]. After this period, the rates of increase slowed down, and, in some cases, the $\Delta E^*$ values were reduced, a phenomenon already described by other researchers [7]. Colour changes in the early phases of ageing may be connected with chromophores present in the paints, most likely as impurities, rather than the ageing procedure [5]. The influence of light was considerable for almost all paint layers, with the FB_G spray paint sample ($\Delta E^*$ = 11.38 SCE and $\Delta E^*$ = 11.02 SCI) exhibiting the most significant colour variation, possibly due to the fact that it contains a mixture of three SOPs (PG7, PY74, PB15:1) and possibly an inorganic pigment rich in Fe. The colours that best resisted solar light aging, as indicated by their small $\Delta E^*$ values, were the white (FB_W > MB_W > MG_W) and black (MG_Bk > MB_Bk > FB_Bk) spray paints, whereas the paints containing synthetic organic pigments were less resistant to photoageing. Furthermore, the pigment PR254 (FB_R sample) proved to be more stable than PR112 (MB_R and MG_R samples). Regarding the green spray paints, it was noticed that PG7 (and PY74) had a greater $\Delta E^*$ shift in Montana Black (5.35/5.81) than in Montana Gold (3.01/3.68) spray paint, indicating that the alkyd binder (MB_B sample) decreases the resistance of spray paint to photoageing to a higher

degree than the acrylic binder (MG_G sample), possibly due to higher photodegradation of the former binder. Noticeable changes in the $\Delta E^*$ values were recorded in the blue spray paints, in which the FB_B sample had the lowest $\Delta E^*$ value (2.09/2.11) compared with both MG_B (2.31/2.21) and MB_B (4.35/4.22) samples. In this case, the different Cu polymorphs present in the spray paints (FB_B, PB15:1/MB_B, and MG_B, PB15: 6) do not seem to affect the photoageing resistance. Finally, the $\Delta h^\circ$ values obtained were negative in the majority of cases, except for those which exhibited a positive $h^*$ shift (FB_W, FB_Bk, FB_G, MB_W, MB_G, MG_G), suggesting that the colour change was not significant [18].

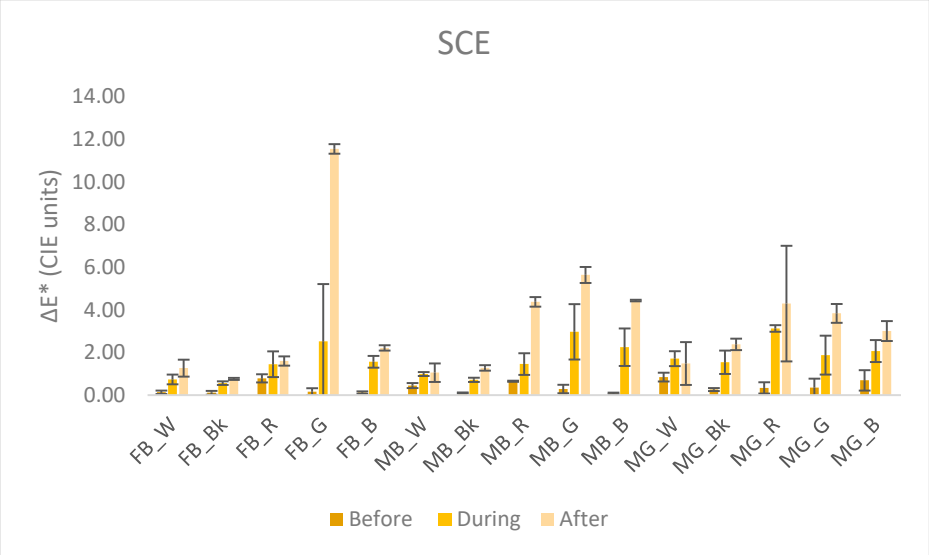


**Chart 2.** $\Delta E^*$ changes of spray paints before (0 h), during (432 h), and after (710 h) their exposure to solar light radiation (SCE mode). Error bars show the standard deviation.

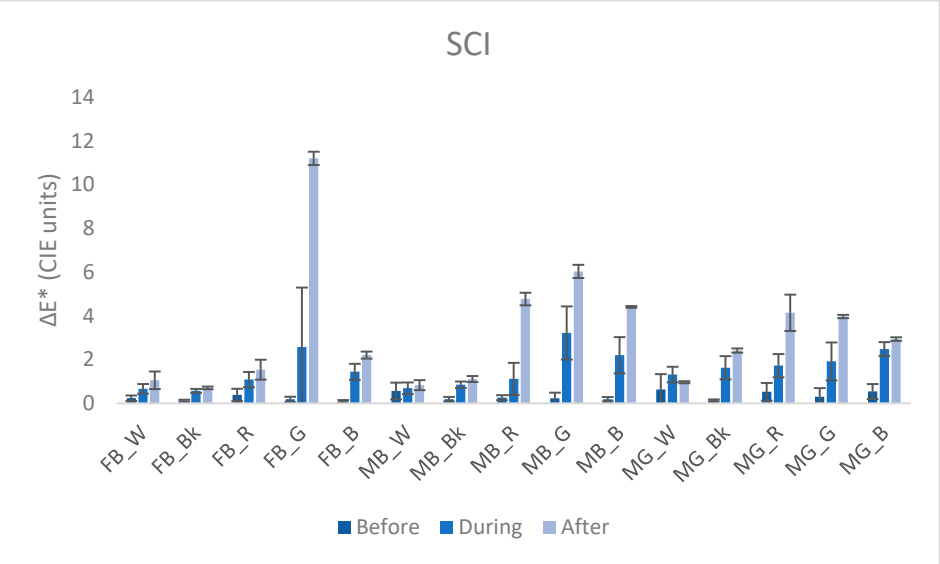


**Chart 3.** $\Delta E^*$ changes of spray paint s before (0 h), during (432 h), and after (710 h) their exposure to solar light radiation (SCI mode).

### *3.4. Gloss Measurement*

Gloss is correlated with surface roughness. In general, rougher surfaces or surfaces with high texture increase the scattering of reflected light, resulting in low gloss values [26]. During the artificial solar light exposure, the gloss values changed remarkably in all spray

paints. Specifically, photoageing resulted in a gloss decrease for Flame Blue spray paints, whereas in Montana Gold spray paints, the gloss increased (Chart 4). The highest $\Delta G$ value was detected in the MG_Bk spray paint (+49 GU), wherein the glossiness was perceptible to the naked eye, while the lowest $\Delta G$ value was detected in the MB_B spray paint (−0.3 GU). The MB_Bk and MB_R spray paints, as well as all the series of Montana Gold spray paints, exhibited a high initial increase in gloss during the first cycles, and then the gloss increase rates were attenuated, remaining higher than the initial gloss value. The glossiness of the MB_W and MB_G spray paints increased at the first exposure dose but decreased at the end of the ageing process and also in comparison with the initial gloss value. Flame Blue spray paints were characterised by a gradual decrease in gloss value. The decrease in gloss may be due to the movement of surfactants on the surface [59]. Finally, the result that the gloss data indicated significant differences between the unaged and aged spray paint samples seems to be in contradiction with the previous result of low SCI and SCE colour changes (which correspond to specular reflectance changes). This inconsistency may be attributed to the BST temperature inside the chamber, which mainly affected the gloss rather than the colour.

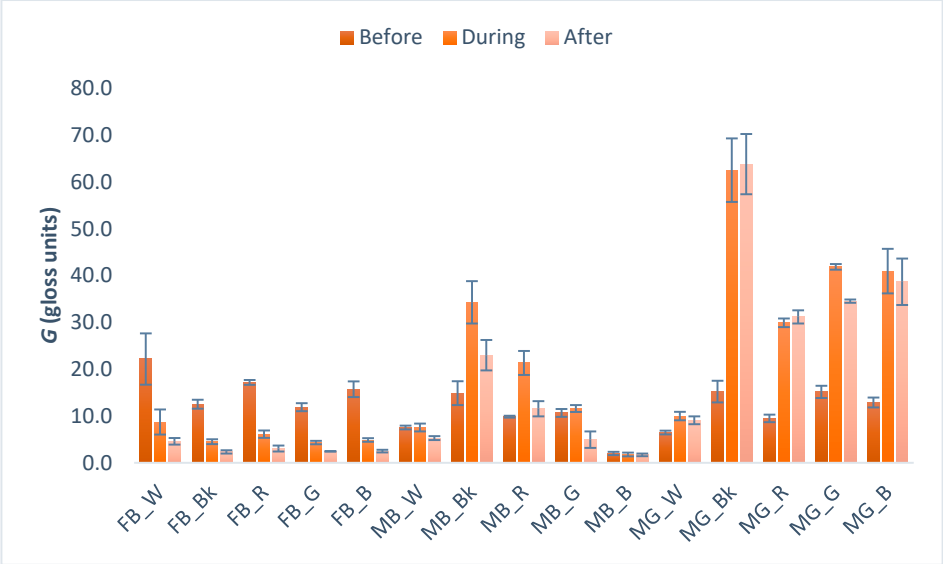


**Chart 4.** Gloss values at 60° before (0 h), during (432 h), and after (710 h) accelerating solar light ageing of the spray paint samples. Error bars show the standard deviation.

### *3.5. Differential Scanning Calorimetry (DSC)*

Regarding the effect of solar light ageing on the thermal behaviour of spray paints, all samples underwent modifications reflecting changes in their thermal properties. All DSC measurements of $T_g$ values of spray paints are shown in Figure 3 and Chart 5. $T_g$ values refer to the height point determination of the endothermic step (baseline shift of the reversing heat flow signal), characterising the glass-to-rubber transition. Since $T_g$ values are indicative that glass transition takes place over a temperature range (and not at a certain temperature) and the $T_g$ of a mixture of various components, as is the case here, is many times difficult to determine, the study of spray paints' thermal behaviour was quite demanding.

First of all, Flame Blue spray paints exhibited the highest $T_g$ values, which were found to be around 50 °C. In contrast, both Montana Black and Montana Gold spray paints had significantly lower $T_g$ values, around 10 °C or lower. The latter (i.e., the low $T_g$ values) is a significant finding, which seems to characterise a large part of these complicated multi-component polymeric systems as the spray paints. Furthermore, this possibly means that the binder amount in Flame Blue spray paints is significantly higher than in both Montana Black and Montana Gold. The higher amount of binder within the spray paint films could

possibly result in a higher impact of solar light ageing on these films. On the other hand, the fact that the $T_g$ values of the acrylic FB spray paints are higher than the ambient temperature (22 °C) in which photoageing takes place will possibly limit the extent of cross-linking photo-oxidative reactions and favour chain-scissions in these films due to low segmental mobility [13]. The opposite (i.e., favouring cross-linking reactions) is expected to happen to both MG and MB paints, which exhibited lower $T_g$ values than the ambient temperature. Second, DSC analysis of almost all spray paints showed a slight increase in $T_g$ values during photoageing indicating, possibly, cross-linking reactions. Photoageing is expected to increase the $T_g$ due to the formation of cross-linked structures [60], and thus, the materials become more brittle and fragile [49]. More specifically, the increase in $T_g$ is associated with the formation of cross-linked structures in the polymeric network affecting the movement of chains in macromolecules. In addition, the loss of organic material by the evaporation of low molecular weight degradation products that act as plasticisers could also occur with a subsequent increase in $T_g$. [49].

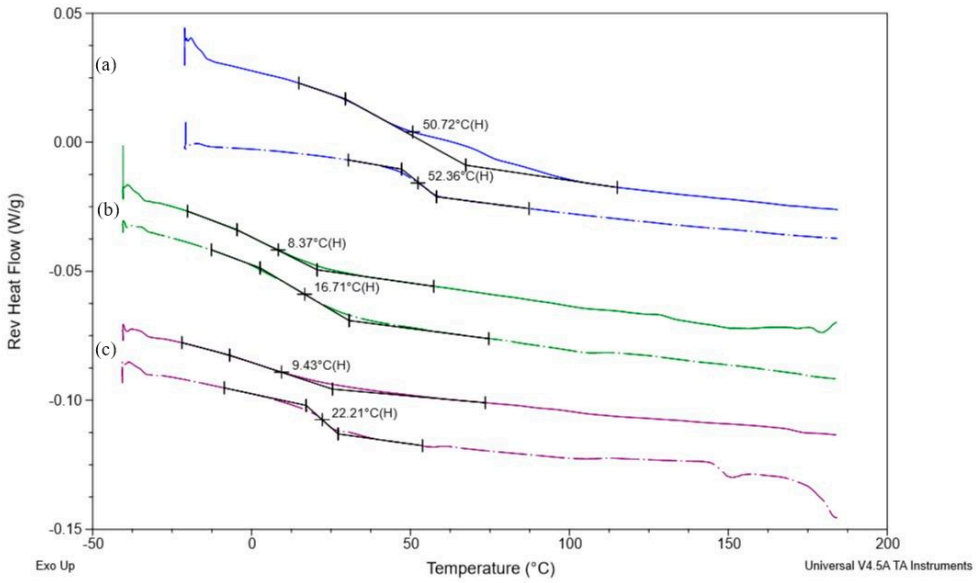


**Figure 3.** Reversing heat flow signal from temperature-modulated DSC of spray paints: (**a**) FB_B, (**b**) MB_G, and (**c**) MG_W. The solid line corresponds to unaged samples, while the short dash line corresponds to the aged ones.

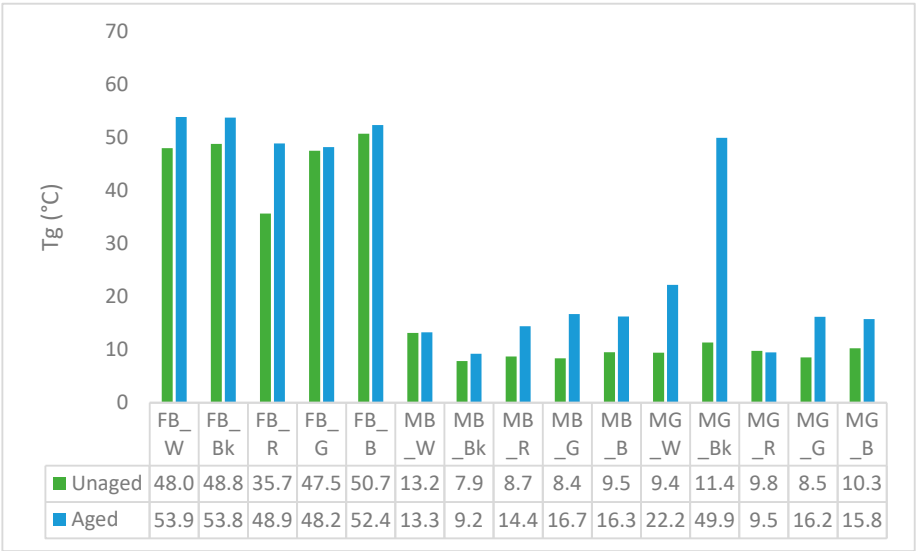


| | FB_W | FB_Bk | FB_R | FB_G | FB_B | MB_W | MB_Bk | MB_R | MB_G | MB_B | MG_W | MG_Bk | MG_R | MG_G | MG_B |
|---|---|---|---|---|---|---|---|---|---|---|---|---|---|---|---|
| Unaged | 48.0 | 48.8 | 35.7 | 47.5 | 50.7 | 13.2 | 7.9 | 8.7 | 8.4 | 9.5 | 9.4 | 11.4 | 9.8 | 8.5 | 10.3 |
| Aged | 53.9 | 53.8 | 48.9 | 48.2 | 52.4 | 13.3 | 9.2 | 14.4 | 16.7 | 16.3 | 22.2 | 49.9 | 9.5 | 16.2 | 15.8 |

**Chart 5.** $T_g$ values of the investigated spray paints before ($t_0$) and after ($t_f$) accelerating solar light ageing.

### *3.6. UV-Vis Spectroscopy*

UV-Vis spectra of both photoaged and unaged spray paint samples were found to be quite informative and in good agreement with those previously reported in the literature. In particular, all UV-Vis spectra showed a decrease in absorption at wavelength > 240 nm (Figure 4a,b). This would suggest either the consumption of chromophores already present in the formulations, probably as impurities [61] or cross-linking reactions and formation of chromophore groups within the polymeric matrix [8]. Moreover, the surface roughness may be correlated to the intensity of the spectra and possibly increase the background of the spectra [8]. Another significant observation made only on the white spray paints is the appearance of a broad absorption band at the visible region between approximately 400 and 700 nm, possibly belonging to the $TiO_2$ since the white spray paints of all companies contain $TiO_2$ in high concentration [39]. Specifically, this band could be attributed to the intra-electron transfer between adjacent metal ions of $TiO_2$ [62,63] indicating possibly that initially, $TiO_2$ is in a reduced state in these spray paints. Interestingly, upon solar light ageing of these spray paints, this broad band of $TiO_2$ decreases in intensity, possibly due to evaporation of the low molecular weight photo-oxidation products of the binder and may be due to partial re-oxidation of $TiO_2$. Nevertheless, the whole issue of $TiO_2$ effect on the solar light ageing of spray paints is considered highly significant [64,65] and needs further investigation.

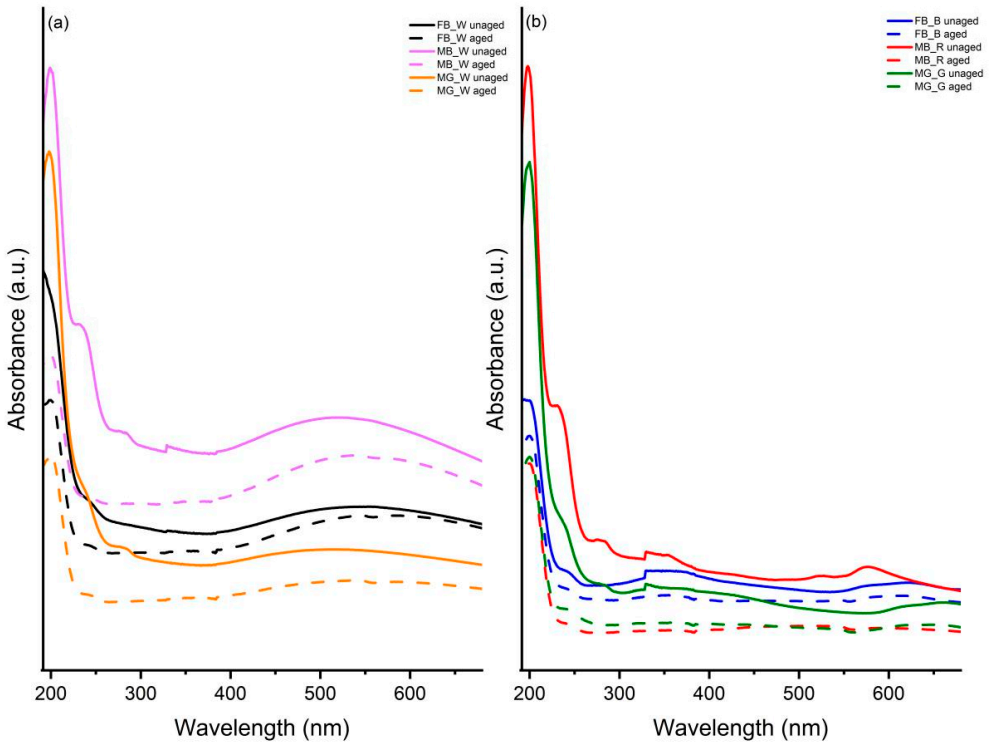


**Figure 4.** UV-Vis spectra of (**a**) white spray paints and (**b**) spray paints of other colours: FB_B, MB_R, and MG_G, before (0 h) and after (710 h) accelerated solar light ageing. The solid line corresponds to unaged samples, while the dashed line to aged samples.

### *3.7. Attenuated Total Reflectance-Fourier Transform Infrared Spectroscopy (ATR-FTIR)—Discussion on Photo-oxidation Reaction Mechanism of Binders*

From the comparison of the IR spectra at various solar light exposure doses, a decrease in the intensity of the polymeric patterns was generally observed. In Figure 5, the spectra of both the unaged and aged black spray paints of the three brands were compared to identify the chemical changes of the binders during solar light ageing.

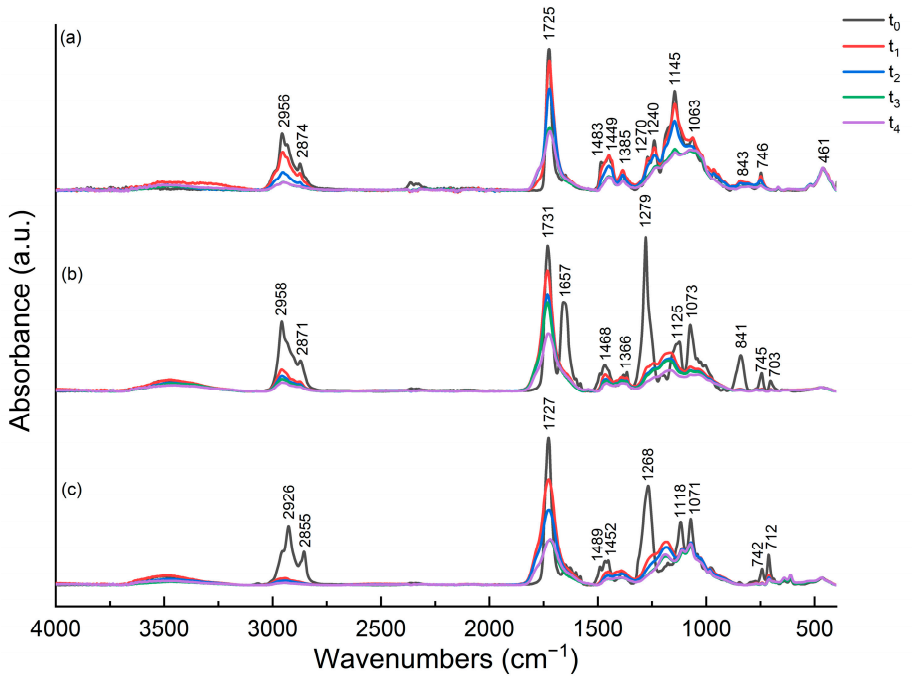


**Figure 5.** ATR-FTIR spectra of the black spray paints: (**a**) FB_Bk, (**b**) MG_Bk, and (**c**) MB_Bk, before (0 h), during (144, 288, 432 h), and after (710 h) accelerated solar light ageing. The spectra have been normalised at ~465 cm$^{-1}$ (Fe oxides), a band that supposedly does not change during photoageing.

#### 3.7.1. ATR-FTIR Study of Flame Blue Binders and Pigments

For the Flame Blue spray paint (Figure 5a), the following spectral changes were observed: slight increase in the OH groups at ca. 3600–3100 cm$^{-1}$, indicating the formation of oxidised species, i.e., alcohol and/or hydroperoxide structures [10,13,25,66]; a progressive decrease in the absorptions in the aliphatic C-H ($CH_2$) stretching region (2956 → 2952 and 2874 → 2879 cm$^{-1}$), possibly due to main-chain scission reactions [10,25]; and progressive decrease, broadening and moderate shift of the C=O carbonyl stretching band to lower wavenumbers (1725 → 1721 cm$^{-1}$) may be attributed to side-chain scission reactions and subsequent removal of the side *n*-butyl ester groups [5,13,25,66]. Especially, the broadening of the C=O band toward lower (1710 cm$^{-1}$) and higher (1780 cm$^{-1}$) wavenumbers is significant and could be linked to the formation of the oxidised species ketones (1710 cm$^{-1}$) and $\gamma$-lactones (1780 cm$^{-1}$), according to a well-known mechanism in the literature (explained below); in contrast, the other possible oxidation products, unsaturated chain ends (1640 cm$^{-1}$) and open chain anhydrides (1800 cm$^{-1}$), could not be detected in the present spectra [13,25,66]. Furthermore, a gradual decrease in the following bands: C-H bending (1449, 1385 cm$^{-1}$) and C-H rocking (747 cm$^{-1}$), which follow the main-chain scission mentioned above was observed. Next, a gradual decrease in the bands in the region of C–O ester groups stretching at 1240 → 1226 and 1145 → 1143 cm$^{-1}$, as well as the C–C stretching band at 965 cm$^{-1}$, was noticed, corroborating the previous assignment for the removal of side *n*-butyl ester groups. Especially for the C–C stretching band at 1063 cm$^{-1}$ (unaged sample), a decrease and shift to higher wavenumbers at 1073 cm$^{-1}$ was observed. However, a contribution to this band could also be attributed to inorganic fillers such as barium sulfate (Learner 2004), which may have migrated to the surface. The gradual decrease in the polymer bands in the fingerprint region (1400–700 cm$^{-1}$) indicates the volatilisation of low molecular weight material formed during the degradation process [5,67]. Additionally, the bands at 1483 (C-H bending), 1270, 1022, and 947 cm$^{-1}$ (C–O and C–C stretching) disappeared almost completely.

From the above FTIR changes of the FB spray paint, it is apparent that the photooxidation of the main binder (*n*BMA-MMA) is mainly caused by the oxidation and chain scission mechanisms well-known in the literature [10,13]. In this mechanism, from the

photo-oxidation and loss of the side *n*-butyl ester groups tertiary macroradicals are formed, which macroradicals can give scission reactions with the production of unsaturated chain ends (tailing at 1640 $cm^{-1}$). The tertiary macroradicals can also be oxidised by molecular oxygen towards hydroperoxides and alcohol groups (3600–3100 $cm^{-1}$) and followed by $\beta$-scission reactions forming ketones (1710 $cm^{-1}$) and low molecular weight products, or the macroradicals can react with adjacent ester groups towards $\gamma$-lactones (1780 $cm^{-1}$). In our case, the formation of alcohols and hydroperoxides as well as the formation of ketones and $\gamma$-lactones is evident. In contrast, the formation of carboxylic acids (1700 $cm^{-1}$) and anhydrides (1800 $cm^{-1}$) is not observed as expected since they are usually formed at high exposure doses [10,13].

Furthermore, a significant decrease in the main absorptions related to nitrocellulose (1651, 1270, 1063, and 843 $cm^{-1}$) was detected, some of which (absorptions) eventually disappeared. This degradation process, known as de-nitration [3], was already observed after the first 144 h of solar light irradiation. In particular, after 710 h of irradiation, the band at 837 $cm^{-1}$ appears to be the only indication of nitrocellulose. Nitrocellulose is also seen in the FB_W at 841 $cm^{-1}$, FB_G at 842 $cm^{-1}$, and FB_B at 841 $cm^{-1}$. Remarkably, in the sample FB_R, the bands of the red pigment and nitrocellulose coincide, so they may appear unaffected. It seems possible that the red pigment (PR254) of the FB_R sample may act as a photostabiliser for NC, i.e., by absorbing light and preventing the photodegradation of NC [17]. The bands related to the SOPs (PR254, PY74, PG7, PB15:1) (Figure 6a) are present but less intense at the end of the photoageing process.

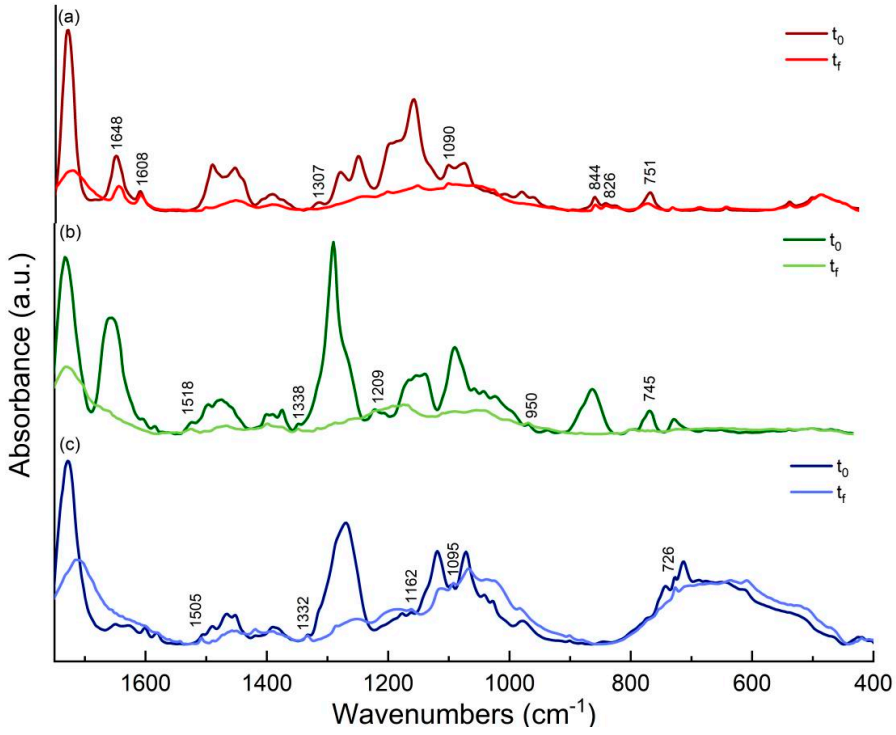


**Figure 6.** Part of ATR-FTIR spectra (1800–400 $cm^{-1}$) of the (**a**) red Flame Blue spray paint, (**b**) green Montana Gold spray paint, and (**c**) blue Montana Black spray paint before (0 h) and after (710 h) accelerated solar light ageing. The spectra have been normalised at 465 $cm^{-1}$ (Fe oxides; FB_R and MG_G) or 675 $cm^{-1}$ ($TiO_2$; MB_B), supposing that these two peaks do not change during photoageing.

### 3.7.2. ATR-FTIR Study of Montana Gold Binders and Pigments

The same degradation pattern of the binding media occurs for the Montana Gold spray paints (Figure 5b), as suggested by the decrease in the intensity of the absorption bands, although to a lesser extent compared with the rest of the companies investigated. The spectra reveal a slight increase in the 3600–3100 $cm^{-1}$ range ascribed to OH stretching, due

to possible photo-oxidative reactions [15]. Furthermore, a gradual decrease in the intensity of the CH stretching bands at 2958 → 2955 and 2871 → 2875 $cm^{-1}$ was recorded. Also, broadening and shift of the carbonyl band to lower wavenumbers (1731 → 1728 $cm^{-1}$) was observed. Additionally, an overall decrease in the main absorptions and loss of resolution in the fingerprint region was observed. In particular, the bands at 1381 → 1387, 1279 → 1240 (sh.), and 1073 → 1071 $cm^{-1}$ corresponding to C-H bending and C-O and C-C stretching, respectively, progressively decreased. The bands at 1125, 1027, and 946 $cm^{-1}$ eventually disappeared. Equally, in this case, the intense nitrocellulose component suffered severe degradation even from the first photo-oxidation stages (144 h). Bands of very low intensity attributed to NC were evident at MG_W, MG_Bk, and MG_B spectra. Styrene exhibited a decrease in the intensity of its characteristic bands, especially in the aromatic skeletal ring vibrations (1599, 1581, and 1489 $cm^{-1}$ not present at the end of photoageing), which (decrease) provides evidence of phenyl ring-opening reactions [5,15]. The aromatic C-H out-of-plane bending bands (745 and 703 $cm^{-1}$) of styrene were decreased, but they were still detectable at the end of the solar light exposure at 743 and 700 $cm^{-1}$ [5]. The bands of the pigments (PR112, PY74, PG7, and PB15:6) were detectable in the ATR-FTIR spectra (Figure 6b) and considered to decrease as compared with the unaged samples. However, due to the photodegradation of the NC it was possible to identify some bands of the PY74 pigment (1672, 1509, and 1227 $cm^{-1}$), which (bands) were not evident in the unaged sample. Finally, it is worth noting an important observation. The 2800–3000 $cm^{-1}$ FTIR region of the MG samples resembles the corresponding region of the FB samples (acrylic binder), whereas the below 2000 $cm^{-1}$ FTIR region of the MG samples resembles the corresponding region of the MB samples (alkyd binder; please see below). This possibly means that the acrylic binder of the MG samples according to our previous work [39] and Table 1 may also contain an alkyd binder, an observation that seems to be reinforced by the subsequent Py-GC/MS study. The whole issue needs further investigation.

#### 3.7.3. ATR-FTIR Study of Montana Black Binders and Pigments

The IR spectra recorded from the Montana Black spray paint at different times of photoageing (Figure 5c) show a progressive decrease in the intensity of the characteristic bands of the alkyd binder. In particular, a small increase in absorption in the whole hydroxyl region between 3600 and 3100 $cm^{-1}$ was observed due to photo-oxidation of the oil component of the alkyd resin and the formation of hydroxyl-bearing species. Furthermore, there was a progressive decrease and shift to higher wavenumbers of the bands ascribed to the C-H stretching region. Specifically, the (C-H) $CH_2$ asymmetric and symmetric stretching bands of the unaged sample at 2956 (sh.), 2926, and 2855 $cm^{-1}$, respectively, shifted to 2972 and 2939 $cm^{-1}$, a phenomenon attributed possibly to hydrogen abstraction mainly as a result of photo-oxidation of the oil portion [7,21,24,68]. Moreover, there was a decrease in intensity, broadening, and shift of the band assigned to C=O carbonyl stretching to lower wavenumbers (1727 → 1719 $cm^{-1}$) due to photo-oxidation [25]. Specifically, the decrease and broadening of the carbonyl band may be due to the formation of low molecular weight, volatile products, such as ketones, aldehydes, and carboxylic acids at 1720, 1735, and 1710 $cm^{-1}$, respectively [21], although these bands are not clearly distinguishable in the spectra; these volatile products are caused by the $\beta$-scission and Norrish type I reactions of the ester groups of both polyester and oil portions of the alkyd resin [22,24,69]. Additionally, a gradual reduction in the remaining bands at 1452 → 1450 and 1386 → 1389 $cm^{-1}$ (C-H bending), 1118 → 1110, 1071 → 1073 (C-O and C-C stretching), and 772 → 770 $cm^{-1}$ (C-H rocking) was detected, due to the photo-oxidation of both phthalate and oil portions. The C-O-C stretching band at 1268 $cm^{-1}$ (as well as the band at 1028 $cm^{-1}$) related to the phthalate portion of the alkyd resin was not present, perhaps due to Norrish type I reaction and the formation of free phthalic acid [25]. However, these bands are present in the rest of the colours, indicating that SOPs act protectively against the photodegradation of alkyd paints. The presence of nitrocellulose was not detectable after 144 h of solar light irradiation. NC could be recognised by the small band at ca. 830 $cm^{-1}$, again in the red colour of the

group. Furthermore, a progressive decrease in the intensity of the bands of the styrene unit due to C–H out-of-plane bending at 742 → 741 and 712 → 709 $cm^{-1}$ was noticed, while the bands related to the aromatic skeletal ring vibrations (1601, 1581, 1489 $cm^{-1}$, unaged sample) of styrene disappeared for the aged black spray paint; in contrast, for the rest of the colours of this brand the latter bands appeared as small shoulders on the broad carbonyl bands. Lastly, the bands ascribed to SOPs (PR112, PY74, PG7, and PB15:6) were present in the spectra of the aged samples, and they appeared less intense as compared with the corresponding bands of the unaged samples (Figure 6c).

### 3.7.4. ATR-FTIR Study of Fillers

In general, the bands attributed to the fillers were detected in the spectra, though with lower intensity at the end of the photoageing process (Figure 7a,b). Thus, no significant chemical variations of inorganic fillers were observed in the ATR-FTIR spectra, as it is known that solar light ageing does not affect their chemical structure. Indeed, talc was inert to solar light radiation [7] and the same seems to happen to the rest of the fillers, as well. More specifically, in the aged MB_W sample (Figure 7c), the following small changes were observed: a slight increase in the calcium carbonate bands at 1418 and 877 $cm^{-1}$, a small increase in the 1040, 1027, and 984 $cm^{-1}$ bands possibly attributed to kaolinite, talc, and barium sulfate, and the appearance of some additional barium sulfate bands at 633 and 608 $cm^{-1}$. The small increase and shift in the bands of the fillers probably results from the photo-oxidation of the binder, as confirmed by previous analytical techniques and in accordance with the literature [25]. On the contrary, some bands attributed to inorganic pigments have disappeared in the final measurements, such as the 1007 and 917 $cm^{-1}$ kaolin bands in the MG_W sample (Figure 7b). Therefore, accelerated solar light ageing of spray paints seems to have a negligible effect on the chemical structure of the inorganic components of these paints.

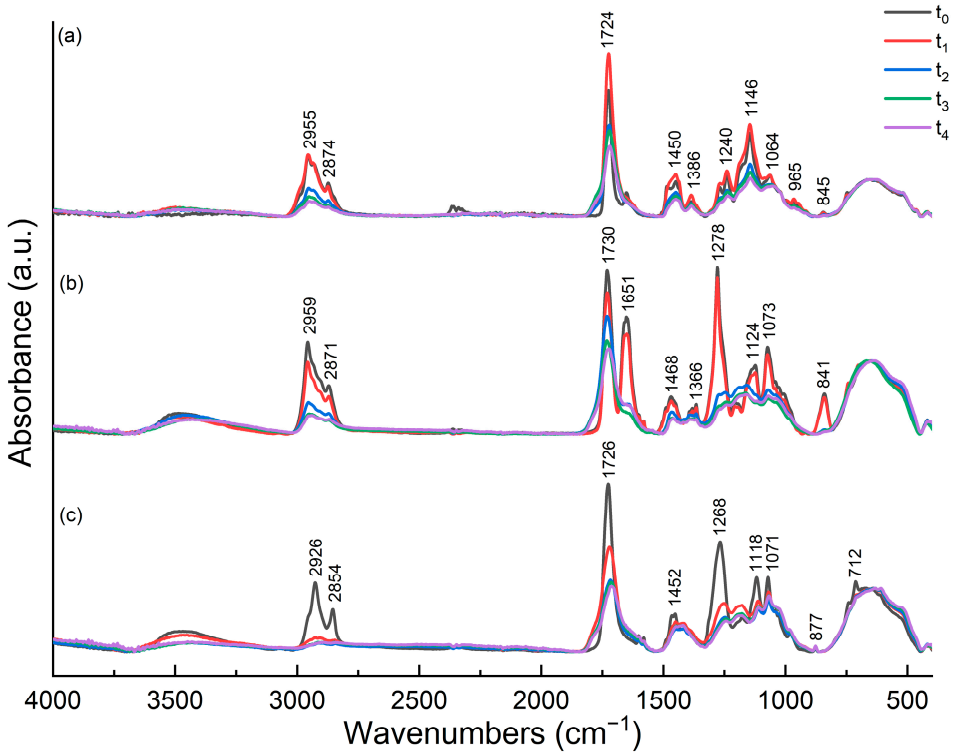


**Figure 7.** ATR-FTIR spectra of the white spray paints: (**a**) FB_W, (**b**) MG_W, and (**c**) MB_W, before (0 h), during (144, 288, 432 h), and after (710 h) accelerated solar light ageing. The spectra have been normalised at 877 $cm^{-1}$ ($CaCO_3$; MB_W) and 670–610 $cm^{-1}$ ($TiO_2$; FB_W and MG_W), supposing that these two peaks do not change during photoageing.

#### 3.7.5. ATR-FTIR Conclusions

To sum up, the acrylic resins were found to be resistant to solar light ageing, showing only small chemical changes (at the specific exposure doses used in this work) in agreement with the literature [1,7,13]. In contrast, alkyd binders, nitrocellulose, and styrene were found to undergo major chemical modifications. On the other hand, synthetic organic pigments and inorganic fillers seem to affect the overall photoactive behaviour of spray paints in a rather small and vague way, except for the red pigment (PR254), which was found to act protectively for the NC as a photostabiliser.

### *3.8. Pyrolysis-Gas Chromatography/Mass Spectrometry (Py-GC/MS)*

Py-GC/MS is a method of analytical chemistry often applied for polymers, where the samples are thermally degraded in the absence of oxygen into smaller and more volatile fragments called pyrolysates. From the chromatograms collected, conclusions are drawn regarding the composition and ingredients of the polymeric samples, as well as ageing degradation mechanisms or thermal endurance of the samples [53]. The method applied each time for the analysis should be the optimum in terms of ingredients identification or intensity of the decomposition reactions. All spray paint samples, both unaged and artificially aged specimens, went through the Py-GC/MS analysis. Figure 8 illustrates all the unaged spray paints as applied in solid form. Differences in the number and shape of peaks are evident depending on the manufacturer, as anticipated; however, they verify the constituents listed in Table 1. In general, both the MB and MG groups of samples elute a higher number of pyrolysates than the FB samples, meaning that there are more organic components in the polymeric matrix of the former. The comprehensive assignment of the various ingredients to the synthesis process entails considerable complexity. However, it is possible to delineate their principal elutants, among which aromatic compounds feature prominently.

More particularly, for FB samples, hydrazine carboxamide is the major elutent at 0.8–1 min; the monomer methyl methacrylate is eluted at 1.8 min, and butyl methacrylate at 3.9 min. This is more or less the case for FB_W, which presents few results, probably due to the high concentration of inorganic pigments. The FB_B and FB_G also contain some polymers with relatively small polymer chains (up to $C_{20}$) other than methacrylates, as proved by the small peaks that appeared after the 15th min. Those small peaks correspond to octadecane (and some derivatives of $C_{18}$), alkenes up to $C_{20}$, monoalcohols ranging from $C_{10}$ to $C_{19}$, esters of 9-hexadecenoic acid, and others. Moreover, the deeper search (NIST Library search) resulted in finding fragments like 4-hydroxybutyric acid hydrazide, isobutyl isothiocyanate, 1-methoxy-2-propyl acetate (PGMEA), *o*-xylene, *N*-ethyl-*n*-butan-4-ol-nitrosamine, trihexyl-silane, and di-*n*-octyl phthalate. Trihexyl-silane may have been used as a coupling agent for adhesion improvement [70], while di-*n*-octyl phthalate (DNOP) has possibly been used as a plasticiser [71]. As far as Figure 8d, which demonstrates the fragmentation results of the red paint FB_R, it is apparent by the curve shape that there is a difference in its elutants. For this colour, the company includes greater quantities of organic compounds, apart from the ingredients mentioned before; the identification yields some extra fragments such as amines [pe. 3-butyl-2,5-dimethyl-piperazine, *N*-(2-methylbutylidene)-2-butylamine, *N*-methylene-n-tetradecylamine], ketones (pe. 3-methyl-cyclopentanone, tetratetracontane, 2-nonadecanone, 2,2-dimethylcyclohexyl methylketone), and some S-compounds (pe. octadecyl 2-pentyl ester of sulfuric acid, thiononyl-lyxofuranoside). As mentioned in Table 1, no aryl hydrocarbons are identified in the pyrolysis products of FB commercial paints.

As far as the MB and MG samples, no great differences in the content of the spray paints (when compared on the basis of their colour) were detected since the basic polymeric matrix looks similar in Figure 8a–d only until the 9–10th min of elution. This may mean that the MG samples also contain an alkyd binder. Later, the height, i.e., intensity, and the plurality of some peaks are different on the chromatograms gathered. It is known that pyrolysis does not affect the inorganic phase of a composite material, which endures higher temperatures. The repetitive sharp and tall peaks at 1.1 min correspond to 2-methylpropanal, while one of the two wide peaks at 9.1- 9.2 min corresponds to phthalic anhydrite for the MB sample.

Phthalic anhydride is the dehydration product from 1,2-benzenedicarboxylic acid (ortho-phthalic acid), which is the principal polybasic acid used in alkyd paints [72]. Those two groups of samples, MB and MG, contain styrenic fragments, which are obvious through their typical triplet of peaks in chromatograms; the monomer styrene is shown at 9 min, the dimmer at 17 min, and the trimer at 21 min of elution [73].

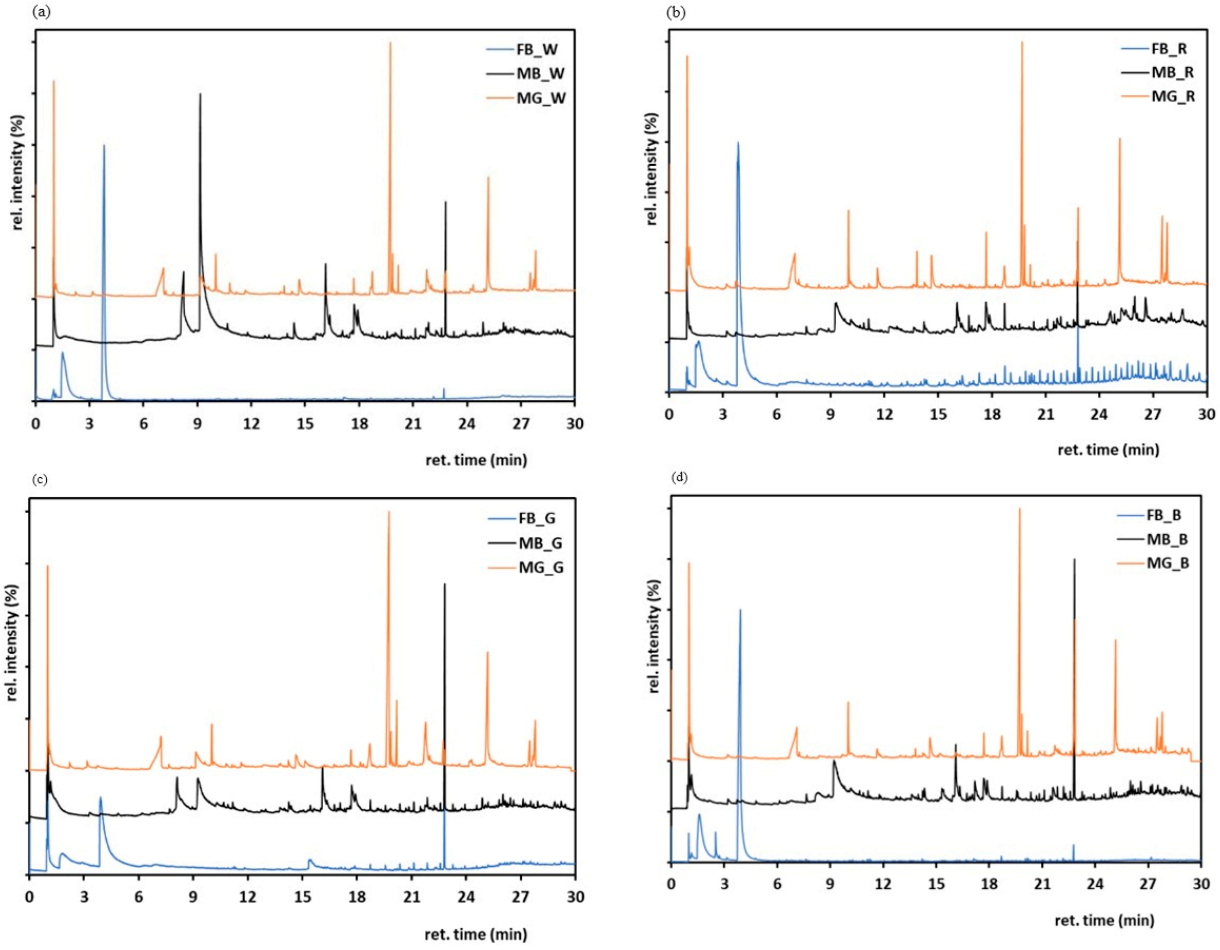


**Figure 8.** Chromatograms of pyrolysates eluted when the unaged samples (**a**) white spray paints, (**b**) red spray paints, (**c**) green spray paints, and (**d**) blue spray paints, obtained from three manufacturers, were pyrolysed at 400 °C.

Regarding the MB samples, apart from the above, other compounds found in high intensities are octacosane, octadecane, 3-methylpentyl pentyl ester of malonic acid, 17-pentatriacontene, di-*n*-octyl phthalate, *N*-Methyl-*N*- benzyltetradecanamine, benzoic acid, 3-hydroxy- butyl ester of butanoic acid, trihexyl-silane, hexadecanoic acid (palmitic), octadecanoic acid (stearic), 1,3-pentanediol, 2,2,4-trimethyl-, and others. Aldehydes are located, too, such as propanal, hexanal, and decanal. The benzoic acid possibly resulted from the decarboxylation of phthalic acid [74]. The long unsaturated compound 17-pentatriacontene has probably been added to the formulation to improve gloss retention properties [6]. Carboxylic acids, such as hexadecanoic acid, octadecanoic acid, octacosanoic acid, and eicosanoic acid, have been added as fluidisation agents, or they may also indicate the presence of metal carboxylates added as dispersion agents [6]. Moreover, octadecanoic acid has also been added as a defoaming agent [75]. 3-butyl-2,5-dimethyl-piperazine was found in MB_R and MB_B samples. Piperazine is probably used as an antimicrobial agent and insect repellent in polymers [76]. MB_R also provided indan-1,2,3-trione (ninhydrin), 2-ethyl-perimidine, lauroyl peroxide. Also, in this case, diethyl adipate has been used as plasticiser, possibly replacing the use of DNOP.

As far as the MG samples, interesting compounds that are identified in high intensities are allyl *n*-octylether, nitrous oxide, 6-methylheptyl-vinylether, 9-hexadecenoic acid, methyl stearate, di-*n*-octyl phthalate, trihexyl-silane, derivatives of oxalic acid, decyl isobutyl ester of manolic acid. Once again, the red paint of the company presents some aromatic amines and cyclic *O*-compounds.

The groups of fragments identified in Py-GC/MS recordings illustrate the degradation processes of the polymeric material, including scission, unzipping, and depolymerisation with monomer production. Two general trends are detected in Figure 9a–c; either there are no great differences between the corresponding unaged and aged samples (MB and MG groups), or fewer peaks are detected in chromatograms of the aged samples compared to the unaged ones (FB group). It is difficult to define exactly the extent of the oxidation of methacrylates occurring during photoageing since 400 °C is a high enough temperature to decompose the methacrylates in whatever form. The volatile compound that is often detected in aged samples is monoammonium salt of carbamic acid ($[NH_4]^+[NH_2CO_2]^-$), found regularly in the paint industry as an organism repellent. However, what we have noticed in the lists of compounds detected is the greater presence of alcohols and substituted alcohols in aged recordings, such as butanols, hexanols, octanols, and 2,4-dimethyl-2,3-pentanediol, along with the fragments already detected in each case. Obviously, alcohols are the main photo-oxidation products of acrylic and alkyd binders investigated in this work, possibly along with aldehydes and/or carboxylic acids. Furthermore, an increase in short-chain products (2-octene and hexanal) in MB samples was observed. This is more or less the case for MB and MG groups of aged samples, which present many elutants in chromatograms. FB_W additionally gave methyl stearate and methyl phaseate at the 17–18th min of elution for the pyrolysed aged sample, while FB_G yielded dithianone at 24.2 min. Again, the specimen FB_R deserves to be further investigated because of its differentiation regarding the fragments of substituted piperidines, pyrroles, aziridines, and pirymidines it elutes.

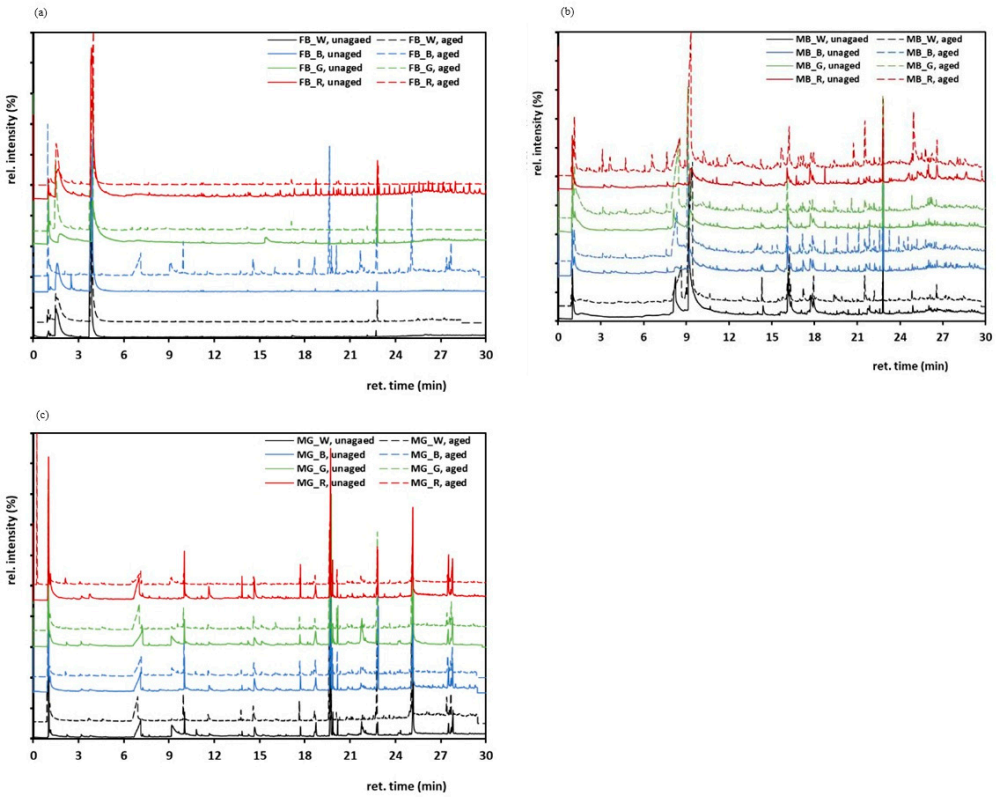


**Figure 9.** Chromatograms of pyrolysates eluted when both unaged and photoaged spray paint samples obtained from three manufacturers: (**a**) FB company, (**b**) MB company, and (**c**) MG company, were pyrolysed at 400 °C. The aged samples are illustrated with the dashed lines in direct comparison with the unaged corresponding samples.

After accelerated solar light ageing, characteristic fragments of SOPs and further additives were detected. In particular, benzenamine, 2-methoxy- and benzene, 1-isocyanato-2-methoxy- found in FB_G are ascribed to PY74 [74]. Diisooctyl adipate (DIOA) eluted in MB_B could suggest the presence of another plasticiser [74], while pentaerythritol, which is one of the two main components of alkyd resin [72], was detected in MB_G. Hexanedioic acid, mono(2-ethylhexyl)ester (ADIPOL) used as co-plasticiser [74], was detected in MG samples after accelerated photoageing.

## 4. Conclusions

Although there are many factors (such as compositional inhomogeneity, surface texture, particle size and distribution, film thickness, etc.) that considerably affect the solar light ageing of spray paint films, many significant findings on this matter were attained in the present research work. Thus, the analyses performed on spray paints before (0 h), during (144, 288, 432 h), and after (710 h) artificial solar light irradiation showed significant changes in their physical, thermal, and chemical properties.

Based on microscopic examination and SEM and AFM analyses, some samples, such as MG_B, exhibited a relative enrichment of fillers and/or organic additives on the surface of the aged paints, resulting in increased surface roughness and, consequently, a decrease in gloss. In contrast, other samples, such as MB_Bk, presented smoother surfaces at the end of photoaging, indicating a decrease in roughness and an increase in gloss. Moreover, during the total exposure dose of 710 h of accelerated photoageing, a decrease in contact angle values was observed, indicating an increase in hydrophilicity of almost all samples, possibly due to the formation of new oxygen-containing species and/or the migration of hydrophilic substances to the surface of the paints. In addition, the highest colour variation at the end of photoageing was observed in the FB_G spray paint, whereas the highest glossiness change ($\Delta G$) was detected in the MG_Bk sample. Nevertheless, in general, the colour changes detected after photoageing were low, whereas the glossiness variations were relatively high. This contradiction was possibly attributed to BST within the chamber, which influences glossiness to a greater extent than colour.

Furthermore, the $T_g$ values of FB spray paints were found to be higher than the ambient temperature in which photoageing takes place, significantly limiting the extent of photoageing reactions (especially the cross-linking reactions), whereas the $T_g$ values of both MB and MG spray paints were lower than the ambient temperature. In addition, all $T_g$ values were found to increase upon photoageing, indicating an increase in the brittleness of the films. Regarding UV-Vis spectroscopy, there is evidence that $TiO_2$ in white spray paints initially may be in a reduced state and then re-oxidised during the photoageing process, possibly indicating that a different photoageing mechanism takes place within these spray paints. The latter finding reveals the significant role of $TiO_2$ in the photoageing of spray paints and necessitates a more in-depth investigation of this issue in the near future.

The main results regarding the photodegradation of the binders were obtained by the ATR-FTIR analyses. In particular, the acrylic resins showed small chemical changes (at the specific exposure doses applied) as a result of solar light ageing, in accordance with the literature. In contrast, alkyd resins, nitrocellulose, and styrene presented major chemical modifications, with the latter two having almost disappeared during the first hours (144 h) of solar light exposure. Through a combination of ATR-FTIR with Py-GC/MS, it was found that the FB spray paints used quite different resins (acrylic binder) than the MB (alkyd) and MG spray paints (acrylic binder containing possibly an alkyd component as well). Furthermore, Py-GC/MS showed that the acrylates are easily evident, plus the white paints are simpler systems, while the red paints are enhanced with aromatic *N*-compounds. It is hard to identify oxidised structures of the resins in the artificially aged samples since the pyrolysis degrades them to (substituted) alkenes, alcohols, aldehydes, and carboxylic acids of $C_6$-$C_{20}$ structures in both cases (unaged and aged samples).

**Supplementary Materials:** The following supporting information can be downloaded at https://www.mdpi.com/article/10.3390/heritage7080186/s1, Table S1: Shifts in the values of $L^*$, $a^*$, $b^*$, total colour $E^*$, chroma $\Delta C^*$, hue $\Delta h^\circ$, $\Delta E^*$, and $\Delta E_{tot}{}^*$ in SCE mode of the investigated spray paints before (0 h), during (432 h), and after (710 h) their exposure to solar light radiation; Table S2: Shifts in the values of $L^*$, $a^*$, $b^*$, total colour $E^*$, chroma $\Delta C^*$, hue $\Delta h^o$, $\Delta E^*$, and $\Delta E_{tot}{}^*$ in SCI mode of the investigated spray paints before (0 h), during (432 h), and after (710 h) their exposure to solar light radiation.

**Author Contributions:** V.M.: Conceptualisation, Methodology, Project administration, Investigation, Data curation, Visualisation, Writing—original draft. A.M.D.: Supervision, Investigation, Validation, Writing—review and editing. E.C.V.: Methodology, Data curation, Writing—original draft; D.B.: Investigation; K.P.: Resources, Investigation, Writing—review and editing. D.N.: Investigation, Writing—review and editing. E.G.: Resources, Investigation, Writing—review and editing. S.O.: Investigation, Writing—review and editing. T.S.: Resources, Investigation, Writing—review and editing. S.B.: Supervision, Investigation, Validation, Data curation, Writing—review and editing. Y.F.: Supervision, Investigation, Validation, Writing—review and editing. All authors have read and agreed to the published version of the manuscript.

**Funding:** The research was partially funded by the Special Account for Research Grants, University of West Attica.

**Data Availability Statement:** Data will be available on request.

**Acknowledgments:** Authors are grateful to Athanasios Karabotsos (Special Technical Laboratory Staff, Department of Conservation of Antiquities and Works of Art, UNIWA) for the valuable collaboration on SEM analyses. Varvara Marazioti would like to thank Professor Anastasia Pournou (Department of Conservation of Antiquities and Works of Art, UNIWA) and Pinelopi Banou (Senior Conservator, Conservation Department of General State Archive, Greece) for their support and guidance on ageing procedure and colour measurements, respectively.

**Conflicts of Interest:** The authors declare that they have no known competing financial interests or personal relationships that could have appeared to influence the work reported in this paper.

## References

1. Pozo-Antonio, J.S.; Rivas, T.; González, N.; Alonso-Villar, E.M. Deterioration of graffiti spray paints applied on granite after a decade of natural environment. *Sci. Total Environ.* **2022**, *826*, 154169. [CrossRef]
2. Rivas, T.; Alonso-Villar, E.M.; Pozo-Antonio, J.S. Forms and factors of deterioration of urban art murals under humid temperate climate; influence of environment and material properties. *Eur. Phys. J. Plus* **2022**, *137*, 1257. [CrossRef]
3. Cimino, D.; Lamuraglia, R.; Saccani, I.; Berzioli, M.; Izzo, F.C. Assessing the (In)Stability of Urban Art Paints: From Real Case Studies to Laboratory Investigations of Degradation Processes and Preservation Possibilities. *Heritage* **2022**, *5*, 581–609. [CrossRef]
4. Pintus, V.; Wei, S.; Schreiner, M. Accelerated UV ageing studies of acrylic, alkyd, and polyvinyl acetate paints: Influence of inorganic pigments. *Microchem. J.* **2016**, *124*, 949–961. [CrossRef]
5. Papliaka, Z.E.; Andrikopoulos, K.S.; Varella, E.A. Study of the stability of a series of synthetic colorants applied with styrene-acrylic copolymer, widely used in contemporary paintings, concerning the effects of accelerated ageing. *J. Cult. Herit.* **2010**, *11*, 381–391. [CrossRef]
6. Izzo, F.C.; Balliana, E.; Perra, E.; Zendri, E. Accelerated ageing procedures to assess the stability of an unconventional acrylic-wax polymeric emulsion for contemporary art. *Polymers* **2020**, *12*, 1925. [CrossRef]
7. Alonso-Villar, E.M.; Rivas, T.; Pozo-Antonio, J.S. Resistance to artificial daylight of paints used in urban artworks. Influence of paint composition and substrate. *Prog. Org. Coat.* **2021**, *154*, 106180. [CrossRef]
8. Anghelone, M.; Jembrih-Simbürger, D.; Pintus, V.; Schreiner, M. Photostability and influence of phthalocyanine pigments on the photodegradation of acrylic paints under accelerated solar radiation. *Polym. Degrad. Stab.* **2017**, *146*, 13–23. [CrossRef]
9. Favaro, M.; Mendichi, R.; Ossola, F.; Russo, U.; Simon, S.; Tomasin, P.; Vigato, P.A. Evaluation of polymers for conservation treatments of outdoor exposed stone monuments. Part I: Photo-oxidative weathering. *Polym. Degrad. Stab.* **2006**, *91*, 3083–3096. [CrossRef]
10. Chiantore, O.; Lazzari, M. Photo-oxidative stability of paraloid acrylic protective polymers. *Polymer* **2001**, *42*, 17–27. [CrossRef]
11. Cortea, I.M.; Rădvan, A.; Vasiliu, C.; Puşcaş, N. Preliminary results of accelerated ageing tests on acrylic art paints. *UPB Sci. Bull. Ser. A Appl. Math. Phys.* **2014**, *76*, 215–222. Available online: https://www.scientificbulletin.upb.ro/rev_docs_arhiva/full6f2_394775.pdf (accessed on 15 May 2023).
12. Sanmartín, P.; Pozo-Antonio, J.S. Weathering of graffiti spray paint on building stones exposed to different types of UV radiation. *Constr. Build. Mater.* **2020**, *236*, 117736. [CrossRef]

13. Chiantore, O.; Trossarelli, L.; Lazzari, M. Photooxidative degradation of acrylic and methacrylic polymers. *Polymer* **2000**, *41*, 1657–1668. [CrossRef]
14. Ciccola, A.; Guiso, M.; Domenici, F.; Sciubba, F.; Bianco, A. Azo-pigments effect on UV degradation of contemporary art pictorial film: A FTIR-NMR combination study. *Polym. Degrad. Stab.* **2017**, *140*, 74–83. [CrossRef]
15. Melchiorre Di Crescenzo, M.; Zendri, E.; Sánchez-Pons, M.; Fuster-López, L.; Yusá-Marco, D.J. The use of waterborne paints in contemporary murals: Comparing the stability of vinyl, acrylic and styrene-acrylic formulations to outdoor weathering conditions. *Polym. Degrad. Stab.* **2014**, *107*, 285–293. [CrossRef]
16. Ranby, B.; Rabek, J. *Photodegradation, Photooxidation, and Photostabilization of Polymers*; Wiley: New York, USA, 1975.
17. Turro, N.J. Modern Molecular Photochemistry. The Benjamin/Cummings Publishing Co., Inc.: Menlo Park, CA, USA, 1978.
18. Doménech-Carbó, M.T.; Silva, M.F.; Aura-Castro, E.; Fuster-López, L.; Kröner, S.; Martínez-Bazán, M.L.; Más-Barberá, X.; Mecklenburg, M.F.; Osete-Cortina, L.; Doménech, A.; et al. Study of behaviour on simulated daylight ageing of artists' acrylic and poly(vinyl acetate) paint films. *Anal. Bioanal. Chem.* **2011**, *399*, 2921–2937. [CrossRef]
19. Ploeger, R.; Chiantore, O. Characterization and Stability Issues of Artists' Alkyd Paints. *Smithson. Contrib. Mus. Conserv.* **2012**, *3*, 89–95.
20. Ploeger, R.; Musso, S.; Chiantore, O. Contact angle measurements to determine the rate of surface oxidation of artists' alkyd paints during accelerated photo-ageing. *Prog. Org. Coat.* **2009**, *65*, 77–83. [CrossRef]
21. Duce, C.; Della Porta, V.; Tiné, M.R.; Spepi, A.; Ghezzi, L.; Colombini, M.P.; Bramanti, E. FTIR study of ageing of fast drying oil colour (FDOC) alkyd paint replicas. *Spectrochim. Acta—Part. A Mol. Biomol. Spectrosc.* **2014**, *130*, 214–221. [CrossRef]
22. Cakić, S.M.; Ristić, I.S.; Vladislav, J.M.; Stamenković, J.V.; Stojiljković, D.T. IR-change and colour changes of long-oil air drying alkyd paints as a result of UV irradiation. *Prog. Org. Coat.* **2012**, *73*, 401–408. [CrossRef]
23. Perrin, F.X.; Irigoyen, M.; Aragon, E.; Vernet, J.L. Artificial aging of acrylurethane and alkyd paints: A micro-ATR spectroscopic study. *Polym. Degrad. Stab.* **2000**, *70*, 469–475. [CrossRef]
24. Pagnin, L.; Calvini, R.; Wiesinger, R.; Weber, J.; Schreiner, M. Photodegradation Kinetics of Alkyd Paints: The Influence of Varying Amounts of Inorganic Pigments on the Stability of the Synthetic Binder. *Front. Mater.* **2020**, *7*, 600887. [CrossRef]
25. Anghelone, M.; Stoytschew, V.; Jembrih-Simbürger, D.; Schreiner, M. Spectroscopic methods for the identification and photostability study of red synthetic organic pigments in alkyd and acrylic paints. *Microchem. J.* **2018**, *139*, 155–163. [CrossRef]
26. Ecco, L.G.; Rossi, S.; Fedel, M.; De, F. Color variation of electrophoretic styrene-acrylic paints under field and accelerated ultraviolet exposure. *Mater. Des.* **2017**, *116*, 554–564. [CrossRef]
27. Giacomucci, L.; Toja, F.; Sanmartín, P.; Toniolo, L.; Prieto, B.; Villa, F.; Cappitelli, F. Degradation of nitrocellulose-based paint by Desulfovibrio desulfuricans ATCC 13541. *Biodegradation* **2012**, *23*, 705–716. [CrossRef] [PubMed]
28. Berthumeyrie, S.; Collin, S.; Bussiere, P.O.; Therias, S. Photooxidation of cellulose nitrate: New insights into degradation mechanisms. *J. Hazard. Mater.* **2014**, *272*, 137–147. [CrossRef] [PubMed]
29. Shashoua, Y.; Bradley, S.M.; Daniels, V.D. Degradation of cellulose nitrate adhesive. *Stud. Conserv.* **1992**, *37*, 113–119. [CrossRef]
30. Webster, R.I.; Webster, H.F. Light Induced Degradation of Nitrocellulose Lacquer Thin Films for Conservation of Art Objects. *MRS Adv.* **2017**, *2*, 3951–3957. [CrossRef]
31. Neves, A.; Ramos, A.M.; Callapez, M.E.; Friedel, R.; Réfrégiers, M.; Thoury, M.; Melo, M.J. Novel markers to early detect degradation on cellulose nitrate-based heritage at the submicrometer level using synchrotron UV–VIS multispectral luminescence. *Sci. Rep.* **2021**, *11*, 20208. [CrossRef]
32. Selwitz, C. *Cellulose Nitrate in Conservation: Research in Conservation*; Getty Conservation Institute: Los Angeles, CA, USA, 1988.
33. Koob, S. The instability of cellulose nitrate adhesives. *Conservator* **1982**, *6*, 31–34. [CrossRef]
34. Farmakalidis, H.V.; Boyatzis, S.; Douvas, A.M.; Karatasios, I.; Sotiropoulou, S.; Argitis, P.; Chryssoulakis, Y.; Kilikoglou, V. The effect of $TiO_2$ component on the properties of acrylic and urea-aldehyde resins under accelerated ageing conditions. *Pure Appl. Chem.* **2017**, *89*, 1659–1671. [CrossRef]
35. Whitmore, P.M.; Colaluca, V.G. The natural and accelerated aging of an acrylic artists' medium. *Stud. Conserv.* **1995**, *40*, 51–64. [CrossRef]
36. Sanmartín, P.; Cappitelli, F. Evaluation of Accelerated Ageing Tests for Metallic Non-Metallic Graffiti Paints Applied to Stone. *Coatings* **2017**, *7*, 180. [CrossRef]
37. Pagnin, L.; Guarnieri, N.; Izzo, F.C.; Goidanich, S.; Toniolo, L. Protecting Street Art from Outdoor Environmental Threats: What Are the Challenges? *Coatings* **2023**, *13*, 2044. [CrossRef]
38. Pellis, G.; Bertasa, M.; Ricci, C.; Scarcella, A.; Croveri, P.; Poli, T.; Scalarone, D. A multi-analytical approach for precise identification of alkyd spray paints and for a better understanding of their ageing behaviour in graffiti and urban artworks. *J. Anal. Appl. Pyrolysis* **2022**, *165*, 105576. [CrossRef]
39. Marazioti, V.; Douvas, A.M.; Katsaros, F.; Koralli, P.; Chochos, C.; Gregoriou, V.G.; Boyatzis, S.; Facorellis, Y. Chemical characterisation of artists' spray-paints: A diagnostic tool for urban art conservation. *Spectrochim. Acta—Part A Mol. Biomol. Spectrosc.* **2023**, *291*, 122375. [CrossRef] [PubMed]
40. *ISO 16474-2:2013/Amd 1:2022*; Paints and Varnishes—Methods of Exposure to Laboratory Light sources—Part 2: Xenon-arc Lamps. International Organization for Standardization: Geneva, Switzerland, 2013.

41. Kampasakali, E.; Ormsby, B.; Cosentino, A.; Miliani, C.; Learner, T. A Preliminary Evaluation of the Surfaces of Acrylic Emulsion Paint Films and the Effects of Wet-Cleaning Treatment by Atomic Force Microscopy (AFM). *Stud. Conserv.* **2013**, *56*, 216–230. [CrossRef]
42. de Sá, M.H.; Eaton, P.; Ferreira, J.L.; Melo, M.J.; Ramos, A.M. Ageing of vinyl emulsion paints—An atomic force microscopy study. *Surf. Interface Anal.* **2011**, *43*, 1160–1164. [CrossRef]
43. Sauerbier, P.; Köhler, R.; Renner, G.; Militz, H. Surface activation of polylactic acid-based wood-plastic composite by atmospheric pressure plasma treatment. *Materials* **2020**, *13*, 4673. [CrossRef]
44. *European Standard, EN 15802*; Conservation of Cultural Property-Test Methods-Determination of Static Contact Angle. IEEE: Washington, DC, USA, 2010.
45. *ISO/CIE 11664-4:2019*; Colorimetry—Part4:CIE1976L*a*b*ColourSpace. International Organization for Standardization/International Commission on Illumination: Geneva, Switzerland, 2019.
46. Farbmetrische Bestimmung von Farbmaßzahlen und Farbabständen im angenähert gleichförmigen CIELAB-Farbraum 2007.
47. Brischke, C.; Obermeyer, C.; Mengel, U. Outdoor Performance of Artist Colours. *Restor. Build. Monum.* **2011**, *17*, 91–102. [CrossRef]
48. *ISO 2813:2014*; Paints and Varnishes—Determination of Gloss Values at 20°, 60° and 85°. International Organization for Standardization: Geneva, Switzerland, 2014.
49. Pintus, V.; Ploeger, R.; Chiantore, O.; Wei, S.; Schreiner, M. Thermal analysis of the interaction of inorganic pigments with p(nBA/MMA) acrylic emulsion before and after UV ageing. *J. Therm. Anal. Calorim.* **2013**, *114*, 33–43. [CrossRef]
50. Simon, S.L. Temperature-modulated differential scanning calorimetry: Theory and application. *Thermochim. Acta* **2001**, *374*, 55–71. [CrossRef]
51. Picollo, M.; Aceto, M.; Vitorino, T. 5. UV-Vis spectroscopy. In *Chemical Analysis in Cultural Heritage*; Sabbatini, L., van der Werf, I., Eds.; De Gruyter: Berlin, Germany; Boston, MA, USA, 2020; pp. 99–120. [CrossRef]
52. Doménech-Carbó, M.T. Novel analytical methods for characterising binding media and protective coatings in artworks. *Anal. Chim. Acta* **2008**, *621*, 109–139. [CrossRef]
53. Vouvoudi, E.C.; Tamias, G.A.; Chatzicharistou, E.A.; Achilias, D.S. Thermal Treatment of a Commercial Polycyanoacrylate Adhesive Addressed for Instant Glass Restoration, for Investigating Its Ageing Tolerance. *Macromol* **2023**, *3*, 636–652. [CrossRef]
54. Aguilar-Rodríguez, P.; Mejía-González, A.; Zetina, S.; Colin-Molina, A.; Rodríguez-Molina, B.; Esturau-Escofet, N. Unexpected behavior of commercial artists' acrylic paints under UVA artificial aging. *Microchem. J.* **2021**, *160*, 105743. [CrossRef]
55. Mejía-González, A.; Zetina, S.; Espinosa-Pesqueira, M.E.; Esturau-Escofet, N. Analysis and Characterization of commercial artists' acrylic paints and the influence of UV light on aging. *Int. J. Polym. Anal. Charact.* **2017**, *22*, 473–482. [CrossRef]
56. Fardi, T.; Kampasakali, E.; Terzopoulou, Z.; Pintus, V.; Pavlidou, E.; Schreiner, M. A preliminary study on the physicochemical properties of pigmented Sty/nBA/MMA emulsion films: The effect of thermal ageing. *Polym. Degrad. Stab.* **2018**, *158*, 157–167. [CrossRef]
57. de la Rie, E.R.; Michelin, A.; Ngako, M.; Del Federico, E.; Del Grosso, C. Photo-catalytic degradation of binding media of ultramarine blue containing paint layers: A new perspective on the phenomenon of "ultramarine disease" in paintings. *Polym. Degrad. Stab.* **2017**, *144*, 43–52. [CrossRef]
58. Pozo-Antonio, J.S.; Barral, D.; Herrera, A.; Elert, K.; Rivas, T.; Cardell, C. Effect of tempera paint composition on their superficial physical properties- application of interferometric profilometry and hyperspectral imaging techniques. *Prog. Org. Coat.* **2018**, *117*, 56–68. [CrossRef]
59. Ormsby, B.; Learner, T. Artists' acrylic emulsion paints: Materials, meaning and conservation treatment options. *AICCM Bull.* **2013**, *34*, 57–65. [CrossRef]
60. Lazzari, M.; Scalarone, D.; Malucelli, G.; Chiantore, O. Durability of acrylic films from commercial aqueous dispersion: Glass transition temperature and tensile behavior as indexes of photooxidative degradation. *Prog. Org. Coat.* **2011**, *70*, 116–121. [CrossRef]
61. Lazzari, M.; Chiantore, O. Thermal-ageing of paraloid acrylic protective polymers. *Polymer.* **2000**, *41*, 6447–6455. [CrossRef]
62. Hiskia, A.; Mylonas, A.; Papaconstantinou, E. Comparison of the photoredox properties of polyoxometallates and semiconducting particles. *Chem. Soc. Rev.* **2001**, *30*, 62–69. [CrossRef]
63. Rothenberger, G.; Moser, J.; Grätzel, M.; Serpone, N.; Sharma, D.K. Charge Carrier Trapping and Recombination Dynamics in Small Semiconductor Particles. *J. Am. Chem. Soc.* **1985**, *107*, 8054–8059. [CrossRef]
64. Kemp, T.J.; McIntyre, R.A. Influence of transition metal-doped titanium(IV) dioxide on the photodegradation of polyethylene. *Polym. Degrad. Stab.* **2006**, *91*, 3020–3025. [CrossRef]
65. Shang, J.; Chai, M.; Zhu, Y. Solid-phase photocatalytic degradation of polystyrene plastic with $TiO_2$ as photocatalyst. *J. Solid. State Chem.* **2003**, *174*, 104–110. [CrossRef]
66. Pintus, V.; Schreiner, M. Characterization and identification of acrylic binding media: Influence of UV light on the ageing process. *Anal. Bioanal. Chem.* **2011**, *399*, 2961–2976. [CrossRef] [PubMed]
67. Cocca, M.; Arienzo, L.D.; Orazio, L.D.; Gentile, G.; Martuscelli, E. Polyacrylates for conservation: Chemico-physical properties and durability of different commercial products. *Polym. Test.* **2004**, *23*, 333–342. [CrossRef]
68. Perrin, F.X.; Irigoyen, M.; Aragon, E.; Vernet, J.L. Evaluation of accelerated weathering tests for three paint systems: A comparative study of their aging behaviour. *Polym. Degrad. Stab.* **2001**, *72*, 115–124. [CrossRef]

69. Anghelone, M.; Jembrih-Simbürger, D.; Schreiner, M. Influence of phthalocyanine pigments on the photo-degradation of alkyd artists' paints under different conditions of artificial solar radiation. *Polym. Degrad. Stab.* **2016**, *134*, 157–168. [CrossRef]
70. Werner, R.; Krysztafkiewicz, A.; Dec, A.; Jesionowski, T. Effect of surface modification on physicochemical properties of precipitated sodium- Aluminium silicate, used as a pigment in acrylic dispersion paints. *Dyes Pigment.* **2001**, *50*, 41–54. [CrossRef]
71. Wei, S.; Pintus, V.; Schreiner, M. A comparison study of alkyd resin used in art works by Py-GC/MS and GC/MS: The influence of aging. *J. Anal. Appl. Pyrolysis* **2013**, *104*, 441–447. [CrossRef]
72. Learner, T.J.S. *Analysis of Modern Paints*; Getty Conservation Institute: Los Angeles, CA, USA, 2004.
73. Chrissafis, K.; Pavlidou, E.; Vouvoudi, E.; Bikiaris, D. Decomposition kinetic and mechanism of syndiotactic polystyrene nanocomposites with MWCNTs and nanodiamonds studied by TGA and Py-GC/MS. *Thermochim. Acta* **2014**, *583*, 15–24. [CrossRef]
74. Germinario, G.; van der Werf, I.D.; Sabbatini, L. Chemical characterisation of spray paints by a multi-analytical (Py/GC–MS, FTIR, μ-Raman) approach. *Microchem. J.* **2016**, *124*, 929–939. [CrossRef]
75. Silva, M.F.; Doménech-Carbó, M.T.; Osete-Cortina, L. Characterization of additives of PVAc and acrylic waterborne dispersions and paints by analytical pyrolysis-GC-MS and pyrolysis-silylation-GC-MS. *J. Anal. Appl. Pyrolysis* **2015**, *113*, 606–620. [CrossRef]
76. Jalageri, M.D.; Nagaraja, A.; Puttaiahgowda, Y.M. Piperazine based antimicrobial polymers: A review. *RSC Adv.* **2021**, *11*, 15213–15230. [CrossRef]


**Disclaimer/Publisher's Note:** The statements, opinions and data contained in all publications are solely those of the individual author(s) and contributor(s) and not of MDPI and/or the editor(s). MDPI and/or the editor(s) disclaim responsibility for any injury to people or property resulting from any ideas, methods, instructions or products referred to in the content.